

1 **Using the Classical Model for**
2 **structured expert judgment to**
3 **estimate extremes: a case study of**
4 **discharges in the Meuse River**

5 Accurate estimation of extreme discharges in rivers, such as the Meuse, is
6 crucial for effective flood risk assessment. However, hydrological models
7 that estimate such discharges often lack transparency regarding the
8 uncertainty of their predictions. This was evidenced by the devastating
9 flood that occurred in July 2021 which was not captured by the existing
10 model for estimating design discharges. This article proposes an approach
11 to obtain uncertainty estimates for extremes with structured expert
12 judgment, using the Classical Model. A simple statistical model was
13 developed for the river basin, consisting of correlated GEV distributions for
14 discharges from upstream tributaries. The model was fitted to seven
15 experts' estimates and historical measurements using Bayesian inference.
16 Results fitted to only the measurements were solely informative for more
17 frequent events, while fitting to only the expert estimates reduced
18 uncertainty solely for extremes. Combining both historical observations and
19 estimates of extremes provided the most plausible results. The Classical
20 Model reduced the uncertainty by appointing most weight to the two most
21 accurate experts, based on their estimates of less extreme discharges. The
22 study demonstrates that with the presented Bayesian approach that
23 combines historical data and expert-informed priors, a group of
24 hydrological experts can provide plausible estimates for discharges, and
25 potentially also other (hydrological) extremes, with a relatively manageable
26 effort.

27 **1 Introduction**

28 Estimating the magnitude of extreme flood events comes with considerable
29 uncertainty. This became clear once more on the 18th of July 2021: A flood
30 wave on the Meuse River, following a few days of rain in the Eiffel and
31 Ardennes, caused the highest peak discharge ever measured at Borgharen.
32 Unprecedented rainfall volumes fell in a short period of time (Dewals et al.
33 2021). These caused flash floods with large loss of life and extensive
34 damage in Germany, Belgium, and to a lesser extent also in the Netherlands
35 (TFFF 2021; Mohr et al. 2022). The discharge at the Dutch border exceeded
36 the flood events of 1926, 1993, and 1995. Contrary to those events, this
37 flood occurred during summer, a season that is (or was) often considered

38 less relevant for extreme discharges on the Meuse. A statistical analysis of
39 annual maxima from a fact-finding study done recently after the flood,
40 estimates the return period to be 120 years based on annual maxima, and
41 600 years when only summer half years (April to September) are
42 considered (TFFF 2021). These return periods were derived including the
43 July 2021 event itself. Prior to the event, it would have been assigned higher
44 return periods. The season and rainfall intensity made the event
45 unprecedented with regard to historical extremes. Given enough time, new
46 extremes are inevitable, but with the Dutch flood safety standards being as
47 high as once per 100,000 years (Ministry of Infrastructure and
48 Environment 2016) one would have hoped this type of event to be less
49 surprising. The event underscores the importance of understanding the
50 variability and uncertainty that comes with estimating extreme floods.

51 Extreme value analysis often involves estimating the magnitude of events
52 that are greater than the largest from historical (representative) records.
53 This requires establishing a model that described the probability of
54 experiencing such events within a specific period, and subsequently
55 extrapolating this to specific exceedance probabilities. For the Meuse, the
56 traditional approach is fitting a probability distribution to periodic maxima
57 and extrapolate from it (Langemheen and Berger 2001). However, a
58 statistical fit to observations is sensitive to the most extreme events in the
59 time series available. Additionally, the hydrological and hydraulic response
60 to rainfall during extreme events might be different for more frequently
61 occurring events, and therefore be incorrectly described by statistical
62 extrapolation.

63 GRADE (Generator of Rainfall And Discharge Extremes) is a model-based
64 answer to these shortcomings. It is used to determine design conditions for
65 the rivers Meuse and Rhine in the Netherlands. GRADE is a variant on a
66 conventional regional flood frequency analysis. Instead of using only
67 historical observations, it resamples these into long synthetic time series of
68 rainfall that express the observed spatial and temporal variation. It then
69 uses a hydrological model to calculate tributary flows and a hydraulic
70 model to simulate river discharges (Leander et al. 2005; Hegnauer et al.
71 2014). Despite the fact that GRADE can create spatially coherent results and
72 can simulate changes in the catchment or climate, it is still based on
73 resampling available measurements or knowledge. Hence, it cannot
74 simulate all types of events that are not present in the historical sample.
75 This is illustrated by the fact that the July 2021 discharge was not exceeded
76 once in the 50,000 years of summer discharges generated by GRADE.

77 GRADE is an example where underestimation of uncertainty is observed,
78 but certainly not the only model. For example, Boer-Euser et al. (2017;
79 Bouaziz et al. 2020) compared different hydrological modelling concepts
80 for the Ourthe catchment (considered in this study as well) and showed the
81 large differences that different models can give when comparing more

82 characteristics than only stream flow. Regardless of the conceptual choices,
83 all models have severe limitations when trying to extrapolate to an event
84 that has not occurred yet. We should be wary to disqualify a model in
85 hindsight after a new extreme has occurred. Alternatively, data-based
86 approaches try to solve the shortcomings of a short record by extending the
87 historical records with sources that can inform on past discharges. For
88 example, paleoflood hydrology uses geomorphological marks in the
89 landscape to estimate historical water levels (Benito and Thorndycraft
90 2005). Another approach is to utilize qualitative historical written or
91 depicted evidence to estimate past floods (Brázdil et al. 2012). The
92 reliability of historical records can be improved as well, for example by
93 combining this with climatological information derived from more
94 consistent sea level pressure data De Niel, Demarée, and Willems (2017).

95 In this context, structured expert judgment (SEJ) is another data-based
96 approach. Expert Judgment (EJ) is a broad term for gathering data from
97 judgments based on expertise in a knowledge area or discipline. It is
98 indispensable in every scientific application as a way of assessing the truth
99 or value of new information. *Structured* expert judgment formalizes EJ by
100 eliciting expert judgments in such a way that judgments can be treated as
101 scientific data. One structured method for this is the Classical Model, also
102 known as *Cooke's method* (Roger M. Cooke and Goossens 2008). The
103 Classical Model assigns a weight to each expert within a group (usually 5 to
104 10 experts) based on their performance in estimating the uncertainty in a
105 number of seed questions. These weights are then applied to the experts'
106 uncertainty estimates for the variables of interest, with the underlying
107 assumption that the performance for the seed questions is representative
108 for the performance in the questions of interest. (Roger M. Cooke and
109 Goossens 2008) shows an overview of the different fields in which the
110 Classical Model for structured expert judgment is applied. In total, data
111 from 45 expert panels (involving in total 521 experts, 3688 variables, and
112 67,001 elicitations) are discussed, in applications ranging from nuclear,
113 chemical and gas industry, water related, aerospace sector, occupational
114 sector, health, banking, and volcanoes. Marti, Mazzuchi, and Cooke (2021)
115 used the same database of expert judgments and observed that using
116 performance-based weighting gives more accurate DMs than assigning
117 weights at random. Regarding geophysical applications, expert elicitation
118 has recently been applied in different studies aimed at informing the
119 uncertainty in climate model predictions (e.g., Oppenheimer, Little, and
120 Cooke 2016; Bamber et al. 2019; Sebok et al. 2021). More closely related to
121 this article, Kindermann et al. (2020) reproduced historical water levels
122 using structured expert judgment (SEJ), and G. Rongen, Morales-Nápoles,
123 and Kok (2022a) applied SEJ to estimate the probabilities of dike failure for
124 the Dutch part of the Rhine River.

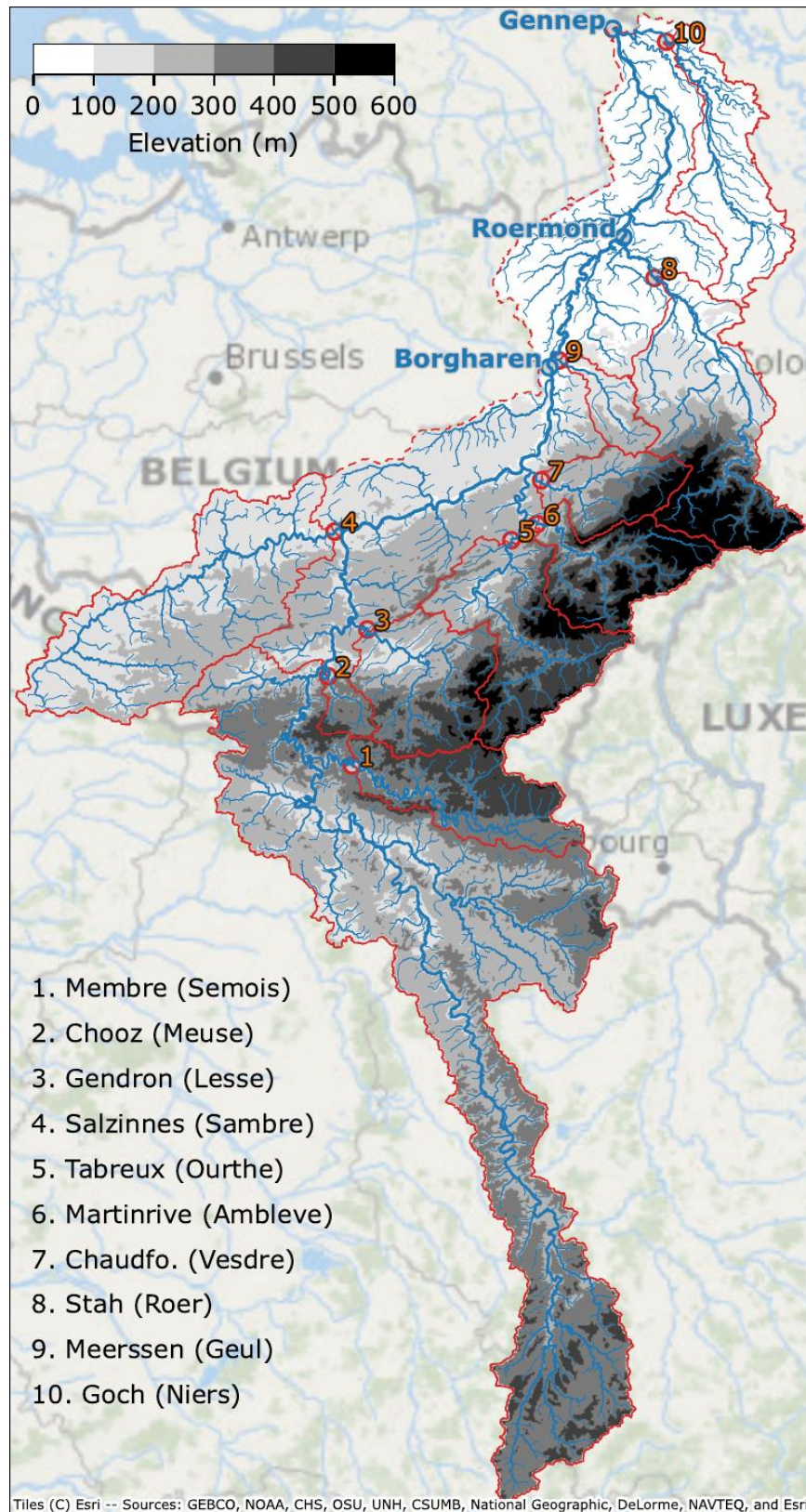
125 While examples of using specifically the Classical Model in hydrology are
126 not abundantly available, there are many examples of expert judgment as
127 prior information to decrease uncertainty and sensitivity. Four examples in
128 which a Bayesian approach, similar to this study, was applied to limit the
129 uncertainty in extreme discharge estimates are given by (Coles and Tawn
130 1996; Parent and Bernier 2003; Renard, Lang, and Bois 2006; Viglione et al.
131 2013). The mathematical approach varies between the different studies, but
132 the rationale for using EJ is the same: adding uncertain prior information to
133 the likelihood of available measurements to help achieve more plausible
134 posterior estimates of extremes.

135 This study applies structured expert judgment to estimate the magnitude of
136 discharge events for the Meuse River up to an annual exceedance
137 probability of on average once per 1,000 years. We aim to get uncertainty
138 estimates for these discharges. Their credibility is assessed by comparing
139 them to GRADE, the aforementioned model-based method for deriving the
140 Meuse River's design flood frequency statistics. A statistical model is
141 quantified both with observed annual maxima and seven experts' estimates
142 for the 10-year and 1000-year discharge on the main Meuse tributaries. The
143 10-year discharges (unknown to experts at the moment of the elicitation)
144 are used to derive a performance-based expert weight that is used to
145 inform the 1000-year discharges. Participants use their own approach to
146 come up with uncertainty estimates. To investigate how the method that
147 combines [1a](#)) data and expert judgments compares to [2b](#)) the data-only or
148 [3c](#)) the expert estimates-only approach, we quantify the model based on all
149 three options. The differences show the added value of each component.
150 This indicates the method's performance both when measurements are
151 available and when they are not, for example in data scarce areas.

152 **2 Study area and data used**

153 Figure 1 shows an overview of the catchment of the Meuse River. The
154 catchments that correspond to the main tributaries are outlined in red. The
155 three locations for which we are interested in extreme discharge estimates,
156 Borgharen, Roermond, and Gennepe, are colored blue. We call these
157 'downstream locations' throughout this study. The river continues further
158 downstream until it flows into the North Sea near Rotterdam. This part of
159 the river becomes increasingly intertwined with the Rhine River and more
160 affected by the downstream sea water level. Consequently, the water levels
161 can be ascribed decreasingly to the discharge from the upstream catchment.
162 For this reason, we do not assess discharges further downstream than
163 Gennepe in this study.

164 The numbered dots indicate the locations along the tributaries where the
165 discharges are measured. These locations' names and the tributaries' names
166 are shown on the lower left.



167

168 *Figure 1: Map of the Meuse catchment considered in this study, with main*
 169 *river, tributaries, streams, and catchment bounds.*

170 Elevation is shown with the grey-scale. Elevation data were obtained from
171 EU-DEM (Copernicus Land Monitoring Service 2017) and used to derive
172 catchment delineation and tributary steepness. These data were provided
173 to the experts together with other hydrological characteristics, like:

- 174 • *Catchment overview*: A map with elevation, catchments, tributaries,
175 and gauging locations
- 176 • *Land use*: A map with land use from Copernicus Land Monitoring
177 Service (2018)
- 178 • *River profiles and time of concentration*: A figure with longitudinal
179 river profiles and a figure with time between the tributary peaks
180 and the peak at Borgharen for discharges at Borgharen greater
181 than 750 m³/s.
- 182 • *Tabular catchment characteristics*, such as: Area per catchment, as
183 well as the catchment's fraction of the total area upstream of the
184 downstream locations. Soil composition from Food and Agriculture
185 Organization of the United Nations (2003), specifying the fractions
186 of sand, silt, and clay in the topsoil and subsoil. Land use fractions
187 (paved, agriculture, forest & grassland, marshes, water bodies).
- 188 • *Statistics of precipitation*: Daily precipitation per month and
189 catchment. Sum of annual precipitation per catchment. Intensity
190 duration frequency curves for the annual recurrence intervals: 1, 2,
191 5, 10, 25, 50, and the maximum. All calculated from gridded E-OBS
192 reanalysis data provided by Copernicus Land Monitoring Service
193 (2020).
- 194 • *Hyetographs and hydrographs*: Temporal rainfall patterns and
195 hydrographs for all catchments/tributaries during the 10 largest
196 discharges measure at Borgharen (sources described below).

197 This information, included in the supplementary information, was provided
198 to the experts to support them in making their estimates. The discharge
199 data needed to fit the model to the observations were obtained from
200 (Service public de Wallonie 2022) for the Belgian gauges, (Waterschap
201 Limburg 2021; Rijkswaterstaat 2022) for the Dutch gauges, and (Land NRW
202 2022) for the German gauge. These discharge data are mostly derived from
203 measured water levels and rating curves. During floods, water level
204 measurements can be incomplete and rating curves inaccurate.
205 Consequently, discharge data during extremes can be unreliable. Measured
206 discharge data were not provided to the experts, except in normalized form
207 as hydrograph shapes.

208 **3 Method for estimating extreme discharges** 209 **with experts**

210 **3.1 Probabilistic model**

211 To obtain estimates for downstream discharge extremes, experts needed to
212 quantify individual components in a model that gives the downstream
213 discharge as the sum of the tributary discharges, times a factor correcting
214 for covered area and hydrodynamics:

$$215 \quad Q_d = f_{\Delta t} \cdot \sum_u Q_u,$$

216 where Q_d is the peak discharge of a downstream location during an event,
217 and Q_u the peak discharge of the u 'th (upstream) tributary during that
218 event. Location d can be any location along the river where the discharge is
219 assumed to be dependent mainly on rainfall in the upstream catchment.
220 The random variable Q_u is modelled with the generalized extreme value
221 (GEV) distribution (Jenkinson 1955). We chose this family of distributions
222 firstly because it is widely used to estimate the probabilities of extreme
223 events. Secondly, it provides flexibility to fit different rainfall-runoff
224 responses by varying between Frechet (heavy tailed), Gumbel (exponential
225 tail) and Weibull distributions (light tailed). We fitted the GEV distributions
226 to observations, expert estimates, or both, using Bayesian inference
227 (described in Sect. 3.3). The factor or ratio $f_{\Delta t}$ in Eq. [eq:main_model]
228 compensates for differences between the sum of upstream discharges and
229 the downstream discharge. These result from, for example, hydraulic
230 properties such as the time difference between discharge peaks and peak
231 attenuation as the flood wave travels through the river (which would
232 individually lead to a factor < 1.0), or rainfall in the Meuse catchment area
233 that is not covered by one of the tributaries (which would individually lead
234 to a factor > 1). When combined, the factor can be lower or higher than 1.
235 The 1,000-year discharge is meant to inform the tail of the tributary
236 discharge probability distributions. This tail is represented by the GEV tail
237 shape parameter that is most difficult to estimate from data. We chose to
238 elicit discharges, rather than a more abstract parameter like the tail shape
239 itself, such that experts make estimates on quantities that may be observed
240 and at "a scale on which the expert has familiarity" (Coles and Tawn 1996,
241 467).

242 The tributary peak discharges Q_u are correlated because a rainfall event is
243 likely to affect an area larger than a single tributary catchment and nearby
244 catchments have similar hydrological characteristics. This dependence is
245 modelled with a multivariate Gaussian copula that is realized through
246 Bayesian Networks estimated by the experts (Hanea, Morales Napoles, and
247 Ababei 2015). The details of this concern the practical and theoretical

248 aspects of eliciting dependence with experts and are beyond the scope of
249 this article. They will be presented in a separate article that is yet to be
250 published. We did use the resulting correlation matrices for calculating the
251 discharge statistics in this study. They are presented in appendix 8.

252 In summary, using the method of SEJ described in Sect. 3.2, the experts
253 estimate

- 254 1. the tributary peak discharges Q_u that are exceeded on average once
255 per 10 years and once per 1,000 years (for brevity called the 10-
256 year and 1,000-year discharge hereafter),
- 257 2. the factor $f_{\Delta t}$, and
- 258 3. the correlation between tributary peak discharges (as explained
259 below).

260 With these, the model in Eq. [eq:main_model] is quantified. The model was
261 deliberately kept simple to ensure that the effect of the experts' estimates
262 on the result remains traceable for them. Section 3.4 explains how
263 downstream discharges were generated from these model components (i.e.,
264 the different terms in Eq. [eq:main_model]), including uncertainty bounds.
265 The model is also described in more detail in (G. Rongen, Morales-Nápoles,
266 and Kok 2022b) as well, where it was used in a data-driven context.

267 **3.2 Assessing uncertainties with using the Classical Model** 268 **for expert judgment judgments**

269 The experts' estimates are elicited using the Classical Model. This is a
270 structured approach to elicit uncertainty for unknown quantities. It
271 combines expert judgments based on empirical control questions, with the
272 aim to find a single combined estimate for the variables of interest (a
273 rational consensus). The Classical Model is typically employed when
274 alternative approaches for quantifying uncertain variables are lacking or
275 unsatisfying (e.g., due to costs or ethical limitations). It is extensively
276 described in (Roger M. Cooke 1991) while applications are discussed in
277 (Roger M. Cooke and Goossens 2008). Here, we discuss the basic elements
278 of the method. We applied the Classical Model because of its strong
279 mathematical base, track record (Colson and Cooke 2017), and the authors'
280 familiarity with this method.

281 In the Classical Model, a group of participants, often researchers or
282 practitioners in the field of interest, provides uncertainty estimates for a set
283 of questions. These can be divided into two categories; seed and target
284 questions. Seed questions are used to assess the participants' ability to
285 estimate uncertainty within the context of the study. The answers to these
286 questions are known by the researchers but not by the participants at the
287 moment of the elicitation. Seed questions are often sourced from similar

288 studies or cases and are as close as possible to the variables of interest. In
289 any case, they are related to the field of expertise of the participant pool,
290 but unknown to the participants. Target questions concern the variables of
291 interest, for which the answer is unknown to both researchers as
292 participants.

293 Because the goal is to elicit uncertainty, experts estimate percentiles rather
294 than a single value. Typically, these are the 5th, 50th, and 95th percentile.
295 Two scores are calculated from an expert's three-percentile estimates; the
296 *statistical accuracy* (SA) and *information* score. The three percentiles create
297 a probability vector with 4 inter-quantile intervals, $p =$
298 $(0.05, 0.45, 0.45, 0.05)$. The fraction of realizations within each of expert e 's
299 inter-quantile interval also forms a four-element vector $s(e)$. $s(e)$ and p are
300 expected to be more similar for an expert e that correctly estimates
301 uncertainty in the seed questions. The statistical accuracy is calculated by
302 comparing each inter-quantile probability p_i to $s_i(e)$. The SA is based on the
303 relative information $I(s(e)|p)$, which equals $\sum_{i=1, \dots, 4} s_i \log(s_i/p_i)$. Using the
304 chi-square test, [\(the quantity \$2 \cdot N \cdot \sum_{i=1, \dots, 4} s_i \log\(s_i/p_i\)\$ is asymptotically](#)
305 [\$\chi^2_3\$ \)](#), the goodness-of-fit between the vectors p and s can be expressed as a
306 p-value. This p-value is used as SA score. The SA is highest if the expert's
307 probability-vector s matches p . For twenty questions, this means the expert
308 overestimates one seed question (i.e., the actual answer was below the 5th
309 percentile), underestimates one question, and has nine questions in both
310 the [5%, 50%] and [50%, 95%] interval. The further away the interquantile
311 ratios s_i/p_i are from 1.0, the lower the SA. [Figure 4 is presented to visualize](#)
312 [the disagreement between \$s_i\$ and \$p_i\$ for this study. This figure will be](#)
313 [further discussed in subsection 4.1. For now, it is sufficient to note that the](#)
314 [agreement between \$s_i\$ and \$p_i\$ is highest for expert D.](#) The statistical accuracy
315 expresses the ability of an expert to estimate uncertainty. Because a
316 variable of interest is uncertain, its realization is considered to be a value
317 sampled from the uncertainty distribution. According to the expert, this
318 realization corresponds to a quantile on the expert-estimated distribution.
319 If an expert manages to reproduce the ratio of realizations within the
320 interquantile intervals (such as in the example with 20 questions above),
321 the probability of the expert being statistically accurate is high, hence they
322 will receive a high p-value. Of course, this match could be coincidental, like
323 any significant p-value from a statistical test. However, in general, a
324 different sample of realizations (in this study, different observed 10-year
325 discharges) is expected to give a p-value (i.e., statistical accuracy) of a
326 similar order.

327 Additional to the SA, the information score compares the degree of
328 uncertainty in an expert's answer compared to other experts. Percentile
329 estimates that are close together (compared to the other participants) are
330 more informative and get a higher information score. The product of the
331 statistical accuracy and information score gives the expert's weight $w_\alpha(e)$:

332 $w_\alpha(e) = 1_\alpha \times \text{statistical accuracy}(e) \times \text{information score}(e)$.

333 The statistical accuracy dominates the expert weight, where the
334 information score modulates between experts with a similar SA. Experts
335 with a SA lower than α can be excluded from the pool by using a threshold,
336 expressed by the 1_α in Eq. [eq:cookes]. This threshold is usually 5%. The
337 (weighted) combination of the experts' estimates is called the decision
338 maker (DM). The experts contribute to the i th item's DM estimate by their
339 normalized weight:

340
$$DM_\alpha(i) = \frac{\sum_e w_\alpha(e) f_{e,i}}{\sum_e w_\alpha(e)}.$$

341 This is called the global weight (GL) DM.

342 Alternatively, ~~the~~ experts can be given the same weight, which results in the
343 equal weight (EQ) DM. This does not require eliciting seed variables, but
344 neither does it distinguish experts based on their performance, a key aspect
345 of the Classical Model. [\(CM\). Roger M. Cooke, Marti, and Mazzuchi \(2021\)](#)
346 [compare GL weights to EQ weights in an out-of-sample cross validation, and](#)
347 [show that using performance-based weights increased the informativeness](#)
348 [of the decision maker estimates by assigning weight to a few experts,](#)
349 [without compromising the DM statistical accuracy \(i.e., the performance of](#)
350 [the DM in 'estimating' uncertainty\).](#)

351 To construct the DM, probability density functions (PDFs) such as $f_{e,i}$ in Eq.
352 [eq:DM], need to be created from the percentile estimates. We used the
353 Metalog distribution for this (Keelin 2016). This distribution is capable of
354 exactly fitting any three-percentile estimate. ~~For symmetric estimates, it is~~
355 ~~bell-shaped. For asymmetric ones~~ [Notice that for this research, the Metalog](#)
356 [distribution represents the uncertainty distribution of each expert over a](#)
357 [particular discharge with a given return period. While it is related to the](#)
358 [underlying distribution of discharge it does not make any assumption about](#)
359 [this underlying distribution other than the ones expressed by experts](#)
360 [through their percentile estimates. For symmetric estimates, the Metalog is](#)
361 [bell-shaped. For asymmetric estimates,](#) it becomes left- or right-skewed.
362 Typically, the Classical Model assumes a uniform distribution in between
363 the percentiles (minimum information). This leads to a stepped PDF where
364 the Metalog gives a smooth PDF. An example of using the Metalog
365 distribution in an expert elicitation study is described by (Dion, Galbraith,
366 and Sirag 2020). All calculations related to the Classical Model were
367 performed using the open-source software ANDURYL (Leontaris and
368 Morales-Nápoles 2018; Hart, Leontaris, and Morales-Nápoles 2019; Guus
369 Rongen et al. 2020).

370 In this study, the seed questions involve the 10-year discharges for the
371 tributaries of the river Meuse. An example of a seed question is: "What is
372 the discharge that is exceeded on average once per 10 years, for the Vesdre

373 at Chaudfontaine?" The target questions concern the 1000-year discharges,
 374 as well as the ratio between the upstream sum and downstream discharge.
 375 Discharges with a 10-year recurrence interval are exceptional but can in
 376 general be reliably approximated from measured data. Seven experts
 377 participated in the in-person elicitation that took place on the 4th of July
 378 2022. The study and model were discussed before the assessments to make
 379 sure that the concepts and questions were clear. After this, an exercise for
 380 the Weser catchment was done in which the experts answered four
 381 questions that were subsequently discussed. In this way, the experts could
 382 compare their answers to the realizations and view the resulting scores
 383 using the Classical Model.

384 Apart from the training exercise, the experts answered 26 questions: 10
 385 seed questions regarding the 10-year discharge (one for each tributary), 10
 386 target questions, regarding the 1,000-year discharge, and 6 target questions
 387 for the ratios between upstream sum and downstream discharge (10-year
 388 and 1,000-year, for three locations). A list of the seven participants' names,
 389 their affiliations, and their field of expertise is shown in Table [\[tab:experts\]](#).
 390 While the participants are pre-selected on their expertise, experts are
 391 scored *post hoc* in terms of their ability to estimate uncertainty in the
 392 context of the study. We note that the alphabetical order of the experts in
 393 the table does not correspond to their labels in the results. An overview of
 394 the data provided to the participants is given in Sect. 2, while the data itself,
 395 as well as the questionnaire, are presented in the supplementary
 396 information.

Name	Affiliation	Field of expertise
Alexander Bakker	Rijkswaterstaat & Delft University of Technology	Risk analysis for storm surge barriers, extreme value analyses, climate change and climate scenario's scenarios .
Eric Sprokkereef	Rijkswaterstaat	Coordinator crisis advisory group Rivers. Operational forecaster for Rhine and Meuse
Ferdinand Diermanse	Deltares	Expert advisor and researcher flood risk.
Helena Pavelková	Waterschap Limburg	Hydrologist
Jerom Aerts	Delft University of Technology	Hydrologist, focussed on hydrologic modelling on a global scale. PhD candidate.
Nicole Jungermann	HKV consultants	Advisor water and climate

397 **3.3 Determining model coefficients with Bayesian**
398 **inference**

399 The model for downstream discharges (Eq. [eq:main_model]) consists of
400 generalized extreme value (GEV) distributions per tributary. The GEV-
401 distribution has three parameters, the location (μ), scale (σ), and shape
402 parameter (ξ). Consider $z = (x - \mu)/\sigma$. The probability density function
403 (PDF) of the GEV is then,

$$404 \quad f(x) = \begin{cases} \frac{1}{\sigma} \exp(-\exp(-z)) \exp(-z), & \text{if } \xi = 0 \\ \frac{1}{\sigma} \exp(-(1 - \xi z)^{1/\xi}) (1 - \xi z)^{1/\xi - 1}, & \text{if } z \leq 1/\xi \text{ and } \xi > 0 \end{cases}$$

405 For each tributary, a (joint) distribution of the model parameters was
406 determined using Bayesian inference, based on expert estimates and
407 observed tributary discharge peaks during annual maxima at Borgharen.
408 Bayesian methods explicitly incorporate uncertainty, a key aspect of this
409 study, and provide a natural way to integrate expert judgment with
410 observed data.

411 Bayes theorem gives the posterior distribution $p(\theta|q)$ of the (hypothesized)
412 GEV-parameters θ given the observed peaks q , as a function of the
413 likelihood $p(q|\theta)$ and the prior distribution $\pi(\theta)$:

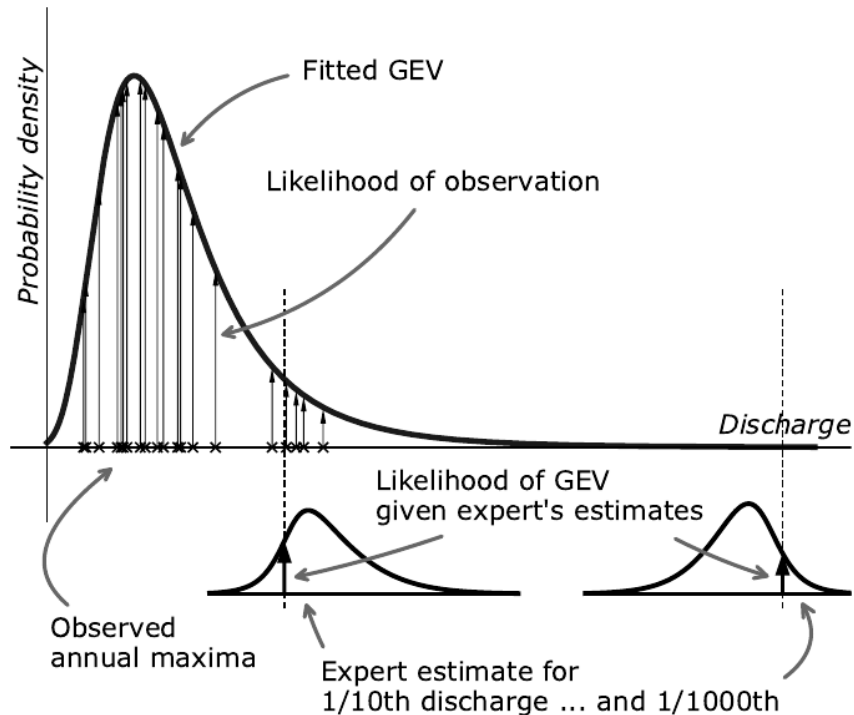
$$414 \quad p(\theta|q) = \frac{p(q|\theta)\pi(\theta)}{p(q)}.$$

415 The likelihood can be calculated using Eq. [eq:GEV_shape_not0] from the
416 product of the probability density of all (independent) annual maxima:
417 $p(q|\theta) = \prod_i (f(q_i|\theta))$. The calculation of the prior is discussed below. That
418 leaves $p(q)$, which is not straightforward to calculate. However, the
419 posterior distribution can still be estimated using the Bayesian sampling
420 technique Markov-Chain Monte Carlo (MCMC). MCMC algorithms compare
421 different propositions of the numerator in Eq. [eq:bayes], leaving the
422 denominator as a normalization factor that crosses out. In this study, we
423 used the affine invariant MCMC ensemble sampler as described by
424 Goodman and Weare (2010), available through the Python module 'emcee'
425 (Foreman-Mackey et al. 2013). This sampler generates a trace of
426 distribution parameters that forms the empirical joint probability
427 distribution of, in our case, the three GEV parameters for each tributary.
428 These are subsequently used to calculate the downstream discharges (see
429 Sect. 3.4).

430 The prior consists of two parts, the expert estimates for the 10-year and
 431 1,000-year discharge, and a prior for the GEV tail shape parameter ξ . Since
 432 the experts do not know the values of the discharges they are estimating,
 433 their estimates can be considered prior information. The prior probability
 434 $\pi(\theta)$ of the expert's estimates is calculated in a similar way as described by
 435 Viglione et al. (2013): Given a GEV-distribution $f(Q|\theta)$, the discharge q for a
 436 specific annual exceedance probability p is calculated from the quantile
 437 function or inverse CDF (F^{-1}),

$$438 \quad q_{p_j} = F^{-1}(1 - p_j|\theta),$$

439 with p_j being the j 'th elicited exceedance probability. This discharge is
 440 compared to the expert's or DM's estimate for this 10- or 1,000-year
 441 discharge, $g(q_{p_j})$. Fig. 2 illustrates this procedure. The top curve $f(Q|\theta)$
 442 represents a proposed GEV-distribution for the random variable Q
 443 (tributary peak discharge) with parameter vector θ . This GEV gives
 444 discharges corresponding to the 0.9 and 0.999th quantile (i.e., the 10-year
 445 and 1,000-year discharge). These discharges can then be compared to the
 446 expert estimates, illustrated by the two bottom graphs. Additionally, the
 447 figure shows the likelihood of observations with the vertical arrows ($p(q|\theta)$)
 448 in Eq. [eq:bayes]).



449

450 *Figure 2: Conceptual visualization of elements in the likelihood-function of a*
 451 *tributary GEV-distribution.*

452 Apart from the expert estimates, we prefer a weakly informative prior for θ
453 (i.e., uninformative, but within bounds that ensure a stable simulation),
454 such that only the data and expert estimates inform the final result.
455 However, an informative prior was added to the shape parameter ξ because
456 with only expert estimates and no data, two discharge estimates are not
457 sufficient for fitting the three parameters of the GEV-distribution.
458 Additionally, the variance in the shape-parameter decreases with
459 increasing number of years (or other block maxima) in a time series
460 (Papalexiou and Koutsoyiannis 2013). The 30 to 70 annual maxima per
461 tributary in this study are not sufficient to reach convergence. [Similar](#)
462 [observations have been presented before for extreme precipitation in](#)
463 [\(Koutsoyiannis 2004a, 2004b\)](#) Therefore, we employ the geophysical prior
464 as presented by Martins and Stedinger (2000); a beta distribution with
465 hyperparameters $\alpha = 6$ and $\beta = 9$ for $x \in [-0.5, 0.5]$, for which the PDF is:

$$466 \quad h(x) = \frac{\Gamma(\alpha + \beta)}{\Gamma(\alpha)\Gamma(\beta)} x^{\alpha-1}(1-x)^{\beta-1},$$

467 with $x = \xi + 0.5$, and Γ being the gamma-function. This PDF is slightly
468 skewed towards negative values of the shape parameter, preferring the
469 heavy tailed Frechet distribution over the light tailed reversed Weibull. In
470 their analysis of a very large number of rainfall records worldwide,
471 Papalexiou and Koutsoyiannis (2013) came to a similar distribution for the
472 GEV-shape parameter. For μ and σ , we assigned equal probability to all
473 values greater than 0. This corresponds to a weakly informative prior for μ
474 (positive discharges), and an uninformative prior for σ (only positive values
475 are mathematically feasible).

476 With both expert estimates g and the constrained tail shape, the prior
477 distribution becomes

$$478 \quad \pi(\theta) = \prod_j \left(g_j \left(F_{\theta}^{-1}(1 - p_j) \right) \right) \cdot h(\xi + 0.5)$$

479 for $-0.5 < \xi < 0.5$, $\sigma > 0$, and $\mu > 0$. $\pi(\theta) = 0$ for any other combination.
480 This gives all the components to calculate the posterior distribution in Eq.
481 [\[eq:bayes\]](#) using MCMC.

482 The posterior distribution comprises the prior tail-shape distribution, the
483 prior expert estimates of the 10-year and 1,000-year discharges, and the
484 likelihood of the observations. As described in Sect. 1 we compare the
485 performance of using data, EJ, and the combination of both. If only data are
486 used, the expert estimates drop out. If only expert judgments are used, the
487 likelihood drops out and both expert estimates are used. If both data and
488 expert judgment are used, only the 1,000-year expert estimate is used.

489 With the just described procedure, the (posterior) distributions for the
490 tributary discharges (Q_u in Eq. [\[eq:main_model\]](#)) are quantified. This leaves

491 the ratio between the upstream sum and downstream discharge ($f_{\Delta t}$) and
 492 the correlations between the tributary discharges to be estimated. For the
 493 ratios, we distinguished between observations and expert estimates as well.
 494 A log-normal distribution was fitted to the observations. This corresponds
 495 to a practical choice for a distribution of positive values with sufficient
 496 shape flexibility. [The ratio itself does not represent streamflow, so there is](#)
 497 [no need to assume a heavy tailed distribution as would be expected for](#)
 498 [streamflow \(Dimitriadis et al. 2021\).](#) The experts estimated a distribution
 499 for the factor as well, which was used directly for the experts-only fit. For
 500 the combined model fit, the observation-fitted log-normal distribution was
 501 used up to the 10-year range, and the expert estimate (fitted with a Metalog
 502 distribution) for the 1,000-year factor. Values of $f_{\Delta t}$ for return periods T
 503 greater than 10 were interpolated (up to 1000-years) or extrapolated,

$$504 \quad f_{\Delta t|T} = f_{\Delta t|10y} + \frac{\log(T) - \log(10)}{\log(1,000) - \log(10)} \cdot (f_{\Delta t|1,000y} - f_{\Delta t|10y}),$$

505 with $f_{\Delta t|10y}$ being sampled from the lognormal and $f_{\Delta t|1,000y}$ from the expert
 506 estimated Metalog distribution. During the expert session, one participant
 507 requested to make different estimates for the factor at the 10-year event
 508 and 1,000-year event, a distinction that initially was not planned. Following
 509 this request, we changed the questionnaire such that a factor could be
 510 specified at both return periods. One expert used the option to make two
 511 different estimates for the factors.

512 Regarding the correlation matrix that describes the dependence between
 513 tributary extremes, the observed correlations were used for the data-only
 514 option and the expert-estimated correlations for the expert-only option. For
 515 the combined option, we took the average of the observed correlation
 516 matrix and the expert-estimated correlation matrix. Other possibilities for
 517 combining correlation matrices are available (see for example Al-Awadhi
 518 and Garthwaite 1998, for a Bayesian approach), however ~~an~~ [in-depth](#)
 519 ~~research~~ [of these options](#) ~~are~~ [beyond](#) the scope of this study.

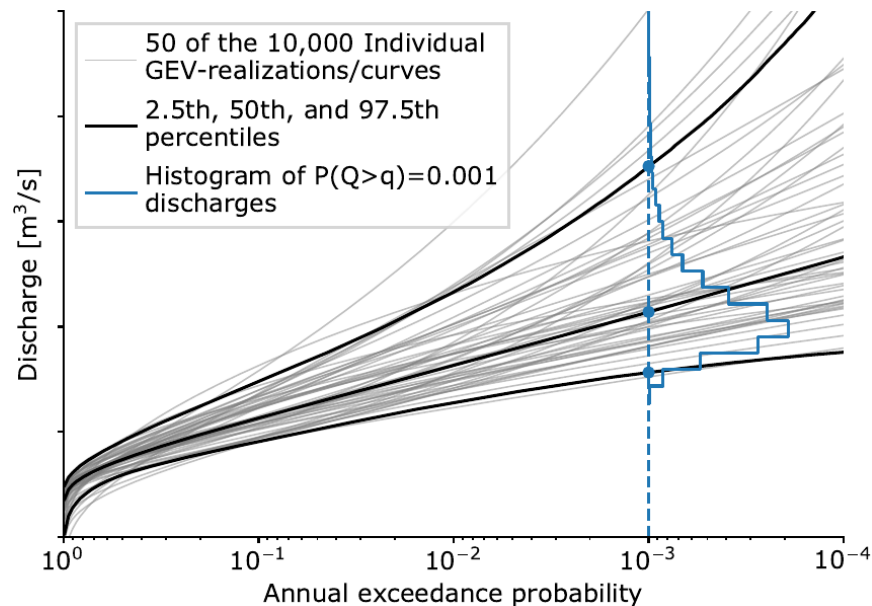
520 **3.4 Calculating the downstream discharges**

521 The three components from Eq. [\[eq:main_model\]](#) needed to calculate the
 522 downstream discharges are:

- 523 • Tributary (marginal) discharges, represented by the GEV-
 524 distributions from the Bayesian inference.
- 525 • The interdependence between tributaries, represented by a
 526 multivariate normal copula.
- 527 • The ratio between the upstream sum and downstream discharges
 528 ($f_{\Delta t}$).

529 In line with the objective of this article, an uncertainty estimate is derived
530 for the downstream discharges. This section describes the method in a
531 conceptual way. Appendix 7 contains a formal step-by-step description.

532 To calculate a single exceedance frequency curve for a downstream
533 location, 10,000 events (annual discharge maxima) are drawn from the 9
534 tributaries' GEV-distributions. Note that 10 tributaries are displayed in Fig.
535 1. The Semois catchment is however part of the French Meuse catchment
536 and therefore only used to assess expert performance. The 9 tributary peak
537 discharges are summed per event and multiplied with 10,000 factors (one
538 per event) for the ratio between upstream sum and downstream discharge.
539 The 10,000 resulting downstream discharges are assigned an annual
540 exceedance probability through empirical plot positions, resulting in an
541 exceedance frequency curve. This process is repeated 10,000 times with
542 different GEV-realizations from the MCMC-trace, resulting in 10,000 curves
543 (each based on 10,000 discharges) from which the uncertainty bandwidth
544 is determined. This is illustrated in Fig. 3. The grey lines depict 50 of the
545 10,000 curves (these can be both tributary GEV-curves, or downstream
546 discharge curves). The (blue) histogram gives the distribution of the 1,000-
547 year discharges. The colored dots indicate the 2.5th, 50th, and 97.5th
548 percentiles in this histogram. Calculating these percentiles for all annual
549 exceedance probabilities results in the black percentile curves, creating the
550 uncertainty interval.



551

552 *Figure 3: Individual exceedance frequency curves for each GEV-realization or*
553 *downstream discharge, and the different percentiles derived from these.*

554 The dependence between tributaries is incorporated in two ways. First, the
555 10.000 events underlying each downstream discharge curve are correlated.
556 This is achieved by drawing the $[9 \times 10,000]$ sample from the (multivariate

557 normal) correlation model, transforming these samples to uniform space
558 (with the normal CDF), and then to each tributary's GEV-distribution space
559 (with the GEV's quantile function). This is the usual approach when
560 working with a multivariate normal copula. The second way of
561 incorporating the tributary dependence is by choosing GEV-combinations
562 from the MCMC-results while considering the dependence between
563 tributaries (i.e., picking high or low curves from the uncertainty bandwidth
564 for multiple tributaries). As illustrated in Fig. 3, a tributary's GEV-
565 distribution can lead to relatively low or high discharges. This uncertainty
566 is largely caused by a lack of realizations in the tail (i.e., not having
567 thousands of years of independent and identically distributed discharges).
568 If one tributary would fit a GEV distribution resulting in a curve on the
569 upper end of the bandwidth, it is likely because it experienced a high
570 discharge event that affected its neighbouring tributary as well.
571 Consequently, the neighbouring tributary is more likely to also have a 'high-
572 discharge' GEV-combination. To account for this, we first sort the GEV-
573 combinations based on their 1,000-year discharge (i.e., the curves'
574 intersections with the blue dashed line), and draw a 9-sized sample from
575 the dependence model. Transforming this to uniform space gives a value
576 between 0 and 1 that is used as rank to select a (correlated) GEV-
577 combination for each tributary. Doing this increases the likeliness that
578 different tributaries will have relatively high or low sampled discharges.

579 **4 Experts' performance and resulting discharge** 580 **statistics**

581 This result section first presents the experts' scores for the Classical Model
582 (Sect. 4.1) and the experts' rationale for answering the questions (Sect. 4.2).
583 After this, the extreme value results for the tributaries (Sect. 4.3) and
584 downstream locations (Sect. 4.4) are presented.

585 **4.1 Results for the Classical Model**

586 The experts estimated three-percentiles (5th, 50th and 95th) for the 10-
587 and 1,000-year discharge for all larger tributaries in the Meuse catchment.
588 An overview of the answers is given in the supplementary material. Based
589 on these estimates, the scores for the Classical Model are calculated as
590 described in Sect. 3.2. The resulting statistical accuracy, information score,
591 and combined score (which, after normalizing, become weights) are shown
592 in table 1.

593 *Scores for the Classical Model, for the experts (top 7 rows) and decision*
594 *makers (bottom 3 rows).*

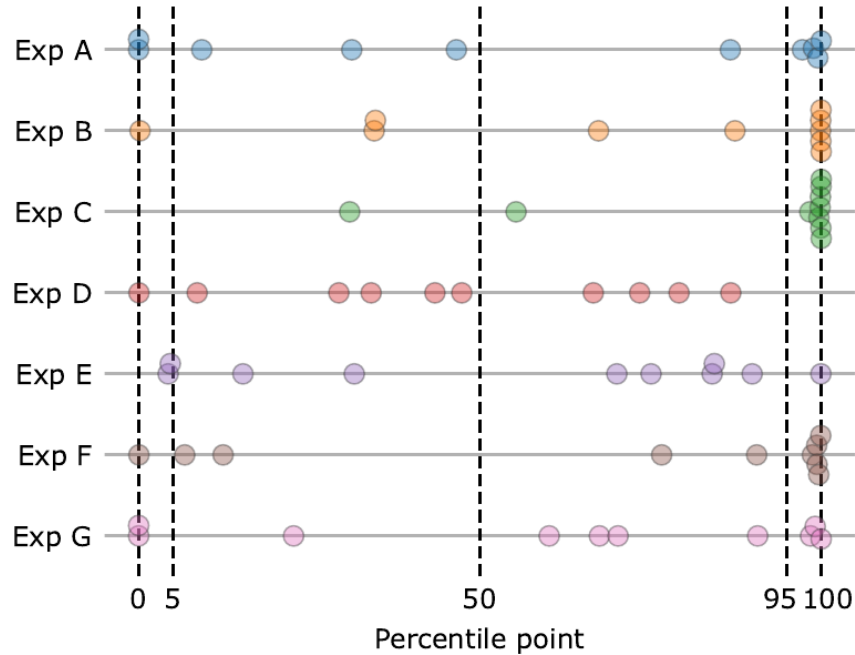
Statistical accuracy Information score Comb. score

		All	Seed	
Exp A	0.000799	1.605	1.533	0.00123
Exp B	0.000456	1.576	1.633	0.000745
Exp C	$2.3 \cdot 10^{-8}$	1.900	1.868	$4.4 \cdot 10^{-8}$
Exp D	0.683	0.711	0.626	0.427
Exp E	0.192	1.395	1.263	0.242
Exp F	0.000456	1.419	1.300	0.000593
Exp G	0.00629	1.302	1.232	0.00775
GL (opt)	0.683	0.659	0.670	0.458
GL	0.683	0.648	0.661	0.452
EQ	0.493	0.537	0.551	0.271

595

596 The statistical accuracy varies between $2.3 \cdot 10^{-8}$ for expert C to 0.683 for
597 expert D. Two experts have a score above a significance level of 0.05. Figure
598 4 shows the position of each realization (answer) within the experts' three-
599 percentile estimate for each of the 10-year discharges. A high statistical
600 accuracy means realizations to these seed variables are distributed
601 accordingly to (or as close to) the mass in each inter-quantile bin: one
602 realization below the 5th percentile, 4 in between the 5th and the median,
603 four between the median and the 95th and one above the 95th. Expert D's
604 estimates closely resemble this distribution ($\frac{1}{10}, \frac{5}{10}, \frac{4}{10}, \frac{0}{10}$ for each inter-
605 quantile respectively), hence the high statistical accuracy score. A
606 concentration of dots on both ends indicates overconfidence (too close
607 together estimates, resulting in realizations outside of the 90% bounds). We
608 observe that most experts tend to underestimate the measured discharges,
609 since most realizations are higher than their estimated 95th percentile.
610 Note that the highest score is not received for the (median) estimates
611 closest to the realization but to evenly distributed quantiles, as the goal is
612 estimating uncertainty rather than estimating the observation (see Sect.
613 3.2).

614 The information scores show, as usual, less variation. The expert with the
615 statistical accuracy (expert D) also has the lowest information score. Expert
616 E, who has a high statistical accuracy as well, estimated more concentrated
617 percentiles, resulting in a higher information score.



618

619 *Figure 4: Seed ~~questions realizations~~ question realizations compared to each*
 620 *expert's estimates. The position of each realization is displayed as percentile*
 621 *point in the expert's distribution estimate.*

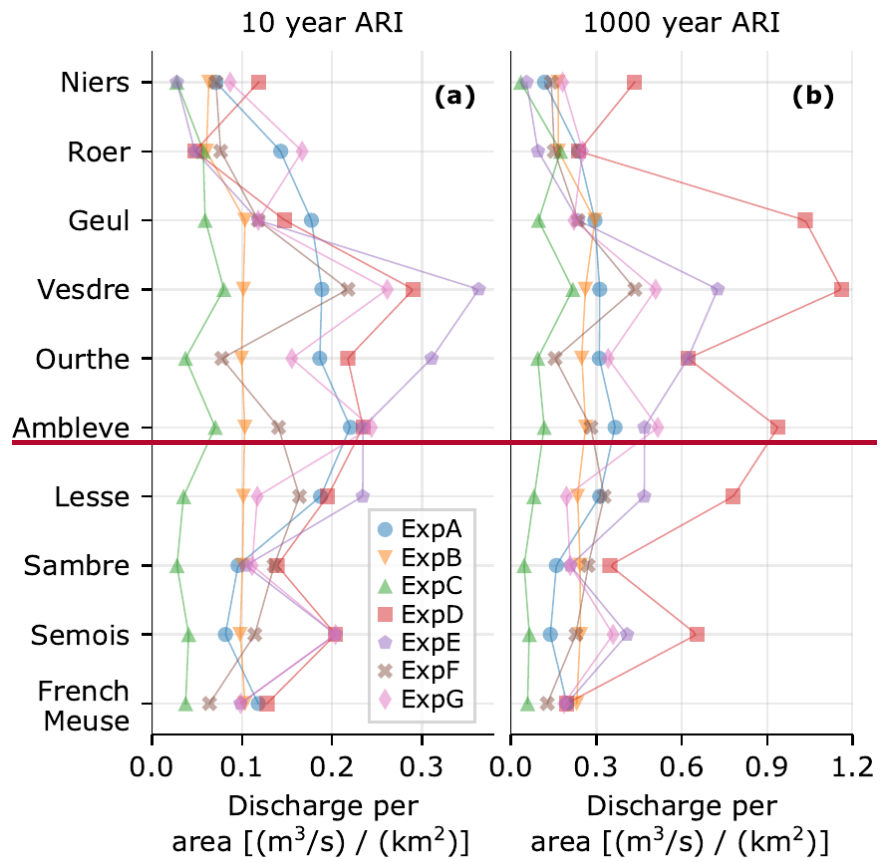
622 The variation between the three decision makers (DMs) in the table is
 623 limited. Optimizing the DM (i.e., excluding experts based on statistical
 624 accuracy to improve the DM-score) has a limited effect. In this case, only
 625 expert D and E would have a non-zero weight, resulting in more or less the
 626 same results compared to including all experts, even when some of them
 627 contribute with 'marginal' weights. The equal weights DM in this case
 628 results in an outcome that is comparable to that of the performance-based
 629 DM, i.e., a high statistical accuracy with a slightly lower information score
 630 compared to the other two DMs.

631 We present the model results as discussed earlier through three cases ~~1a)~~
 632 ~~only data, 2b)~~ only expert estimates, and ~~3c)~~ the two combined as described
 633 in Section 3.3. We used the global weights DM for the data and experts
 634 option ~~3c)~~. This means the experts' estimates for the 10-year discharges
 635 were used to assess the value of the 1,000-year answer. For the experts-
 636 only option, we used the equal weights DM, because using the global
 637 weights emphasizes estimates matching the measured data in the 10-year
 638 range. This would indirectly lead to including the measured data in the fit.
 639 By using equal weights, we ignore the relevant seed questions and the
 640 corresponding differential weights.

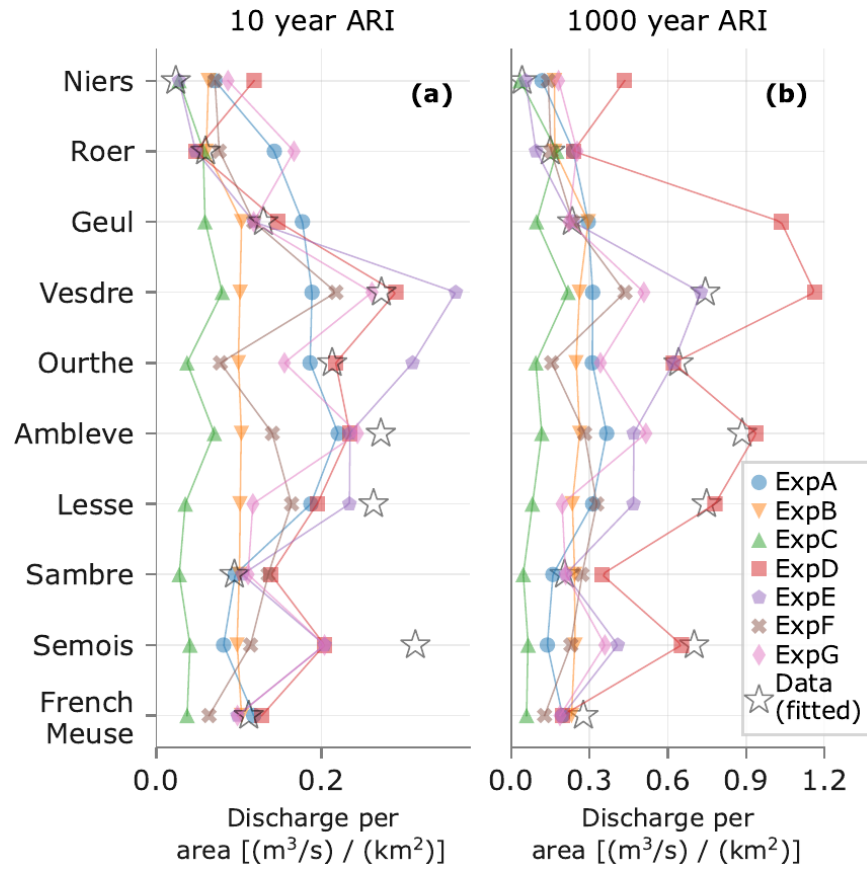
641 **4.2 Rationale for estimating tributary discharges**

642 We requested the experts to briefly describe the procedure they followed
643 for making their estimates. Overall, three approaches were distinguished.
644 The first was using a simple conceptual hydrological model, in which the
645 discharge follows from catchment characteristics like (a subset of) area,
646 rainfall, evaporation and transpiration, rainfall-runoff response, land-use,
647 subsoil, slope, or the presence of reservoirs. Most of this information was
648 provided to the experts, and if not, they made estimates for it themselves. A
649 second approach was to compare the catchments to other catchments
650 known by the expert, and possibly adjusting the outcomes based on specific
651 differences. A third approach was using rules of thumb, such as the
652 expected discharge per square kilometer of catchment or a 'known' factor
653 between an upstream tributary discharge and a downstream discharge (of
654 which the statistics are better known). For estimating the 1,000-year
655 discharge, the experts had to do some kind of extrapolation. Some experts
656 scaled with a fixed factor, while others tried to extrapolate the rainfall, for
657 which empirical statistics were provided. The hydrological data
658 (described in Sect. 2) was provided to the experts in spreadsheets as well,
659 making it easier for them to do computations. However, the time frame of
660 one day (for the full elicitation) limited the possibilities for making detailed
661 model simulations.

662 Figure 5 ~~gives an impression of~~ [shows](#) how the different approaches led to
663 different answers per tributary. It compares the 50th percentile of the
664 discharge estimates per tributary of each expert, by dividing them through
665 the catchment area. ~~From the figure we can see~~ [The 10-year and 1,000-year](#)
666 [discharges from fitting the observations \(i.e., the data only approach\) are](#)
667 [indicated with the stars. The figure shows](#) that most experts estimated
668 higher discharges for the steeper tributaries (Ambleve, Vesdre, Lesse). The
669 experts estimated the median 1,000-year discharges to be 1.7 to 3.8 times
670 as high as the median 10-year discharge, with an average of on average 2.3
671 for all experts and tributaries. The statistically most accurate expert, Expert
672 D, estimated factors in between 1.6 and 7.0. Contrarily, expert E, with the
673 second highest score, estimated a ratio of 2.0 for all tributaries.



674



675

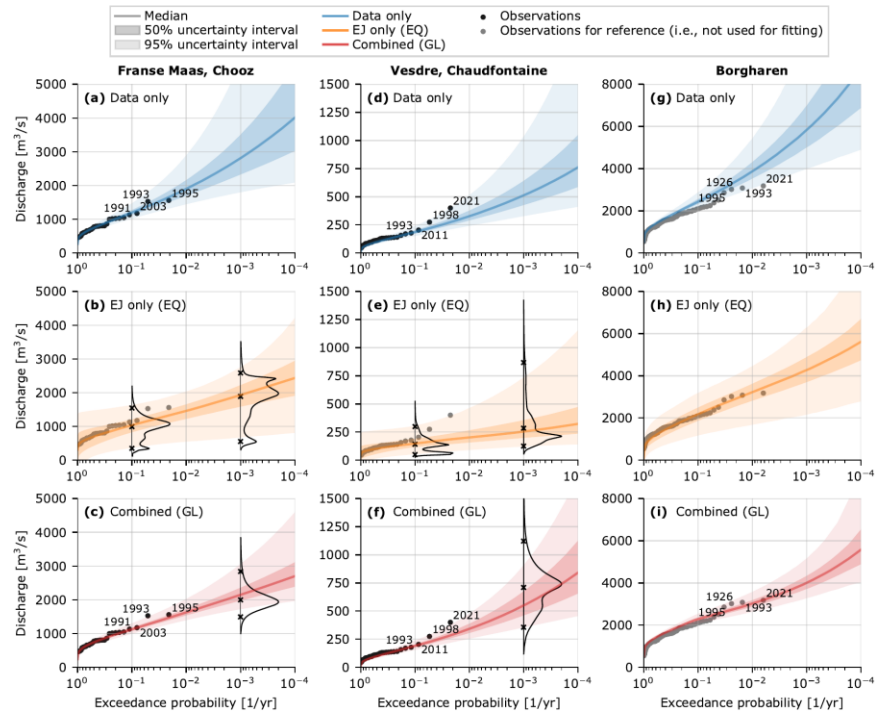
676 *Figure 5: Discharge per area for each tributary and experts, based on the*
 677 *estimate for the 50th percentile. (a) for the 10-year, and (b) for the 1,000-*
 678 *year discharge. Observed or fitted discharges are indicated with stars. The*
 679 *lines are displayed to help distinguish overlapping markers.*

680 For estimating the factor between the tributaries' sum and the downstream
 681 discharge (f_{At} in Eq. [eq:main_model]), experts mainly took into
 682 consideration that not 100% of the area is covered by the tributary
 683 catchments for which the discharge-estimates were made, and that the
 684 tributary hydrograph peaks have different lag times. Additional aspects
 685 noted by the experts were the effects of flood peak attenuation and spatial
 686 dependence between tributaries and rainfall.

687 4.3 Extreme discharges for tributaries

688 We calculated the extreme discharge statistics for each of the tributaries
 689 based on the procedures described in Sect. 3.3. Figure
 690 [fig:extreme_discharges_Borgharen] shows the results for Chooz and
 691 Chaudfontaine (left and middle column). Chooz is a larger not too steep
 692 tributary, while Chaudfontaine is a smaller steep tributary (see figure 1).
 693 The right column shows the discharges for Borgharen, the location where
 694 we want to estimate the discharges through Eq. [eq:main_model], which is

695 further discussed in Sect. 4.4. The results for the other tributaries are
 696 shown in the supplementary information for all experts and DMs.



697

698 The top row (a, d, g) in Fig. [fig:extreme_discharges_Borgharen] shows the
 699 uncertainty interval of these distributions when fitted only to the discharge
 700 measurements. The outer colored area is the 95% interval, the ~~more~~
 701 ~~opaque~~ ~~opaquer~~ inner area the 50% interval, and the thick line the median
 702 value. The second row (b, e, h) shows the fitted distributions when only
 703 expert estimates are used. The bottom row (c, f, i) shows the combination of
 704 expert estimates and data. The data-only option closely matches the data in
 705 the return period range where data are available, but the uncertainty
 706 interval grows for return periods further outside sample. Contrarily, the
 707 experts-only option shows much more variation in the 'in sample' range,
 708 while the out of sample return periods are more constrained. The combined
 709 option is accurate in the 'in sample' range, while the influence of the DM
 710 estimates is visible in the 1,000-year return period range.

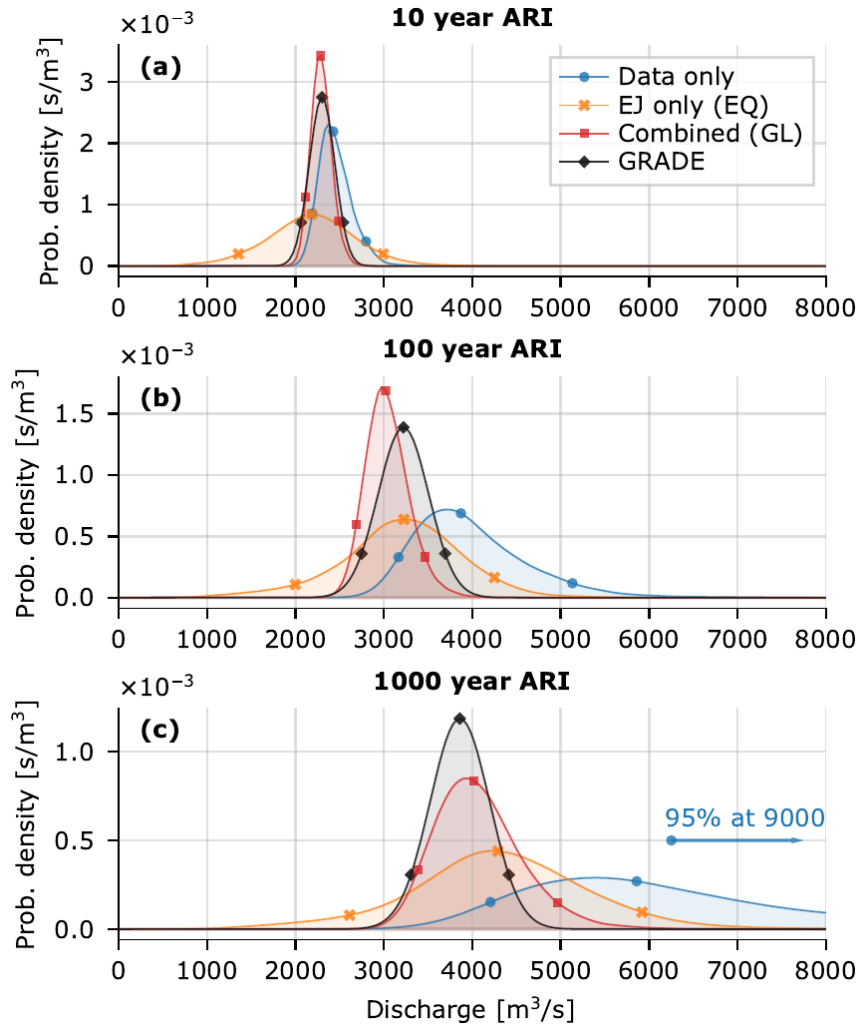
711 4.4 Extreme discharges for Borgharen

712 Combining all the marginal (tributary) statistics with the factor for
 713 downstream discharges and the correlation models estimated by the
 714 experts, we get the discharge statistics for Borgharen. The results for this
 715 are shown in Fig. [fig:extreme_discharges_Borgharen] (g, h, i).

716 As with the statistics of the tributaries, we observe high accuracy for the
 717 data-only estimates in the 'in sample' range, constrained uncertainty
 718 bounds for EJ-only in the range with higher return periods, and both when

719 combined. The combined results match the historical observations well.
720 Note that this is not self-evident as the distributions were not fitted directly
721 to the observed discharges at Borgharen but rather obtained through the
722 dependence model for individual catchments and equation
723 [\[eq:main_model\]](#). Contrarily, the data-only results deviate from the
724 observations in the 10- to 100-year range. Sampling from the fitted model
725 components (GEVs, dependence model, and factors) does not accurately
726 reproduce the downstream discharges in this range because they were
727 individually fitted and not as a whole. We do not consider this a problem, as
728 the study is oriented towards showing the effects of expert quantification in
729 combination with more traditional hydrological modelling. The EJ-only
730 estimates give a much wider uncertainty estimate. The experts' combined
731 median matches the observations surprisingly well, but the large
732 uncertainty within the observed range cautions against drawing general
733 conclusions on this.

734 Zooming in on the discharge statistics for the downstream location
735 Borgharen, we consider the 10, 100, and 1,000-year discharge. Figure 6
736 shows the (conditional) probability distributions (smoothed with a kernel
737 density estimate) for these discharges at the location of interest.



738

739 *Figure 6: Kernel density estimates for the 10-year (a), 100-year (b), and*
 740 *1,000-year (c) discharge for Borgharen. The dots indicate the 5th, 50th and*
 741 *95th percentile.*

742 Comparing the three modelling options discussed thus far, we see that the
 743 data-only option is very uncertain, with a 95% uncertainty interval of 4,000
 744 to around 9,000 m³/s for the 1,000-year discharge. A Meuse-discharge of
 745 4,000 m³/s will likely flood large stretches along the Meuse in the Dutch
 746 province Limburg, while a discharge of 5,000 m³/s also floods large areas
 747 further downstream (GWF Rongen 2016). For discharges higher than 6,000
 748 m³/s the applied model (Eq. [eq:main_model]) should be reconsidered, as
 749 the hydrodynamic properties of the system change due to upstream
 750 flooding.

751 The combined results are surprisingly close to the currently used GRADE-
 752 statistics for dike assessment; the uncertainty is slightly larger, but the
 753 median is very similar. The EJ-only results are less precise, but the median
 754 values are similar to the combined results and GRADE-statistics. The large

755 uncertainty is mainly the results of equally weighting all experts, instead of
756 assigning most weight to experts D and E (as done for the global weight
757 DM). For the combined data and EJ approach, the results for the tributary
758 discharges roughly cover the intersection of the EJ-only and data-only
759 results (see Fig. [fig:extreme_discharges_Borgharen] a-f). Figure 6 does not
760 show this pattern, with the EJ-only results positioned in between the data-
761 only and combined results. This is mainly due to equal weight DM used for
762 the EJ-only results, which gives a higher factor between upstream and
763 downstream discharges ($f_{\Delta t}$ in Eq. [eq:main_model]), and therefore higher
764 resulting downstream discharges. Overall, the combined effect of data and
765 EJ is more difficult to identify in the downstream discharges (Fig.
766 [fig:extreme_discharges_Borgharen] g-i) than it is in the tributary discharge
767 GEVs (Fig. [fig:extreme_discharges_Borgharen] a-f). This is due to the
768 additional model components (i.e., the factor between upstream and
769 downstream, and the correlation model) affecting the results. Additional
770 plots similar to Fig. [fig:extreme_discharges_Borgharen] that illustrate this
771 are presented in the supplementary information. There, the results for the
772 other two downstream locations, Roermond and Gennep, are presented as
773 well. These results behave similar to those for Borgharen and are therefore
774 not presented here.

775 **5 Discussion**

776 This study proposed a method to estimate credible discharge extremes for
777 the Meuse River (1,000-year discharges in the case of this research).
778 Observed discharges were combined with expert estimates through the
779 GEV-distribution, using Bayesian inference. The GEV-distribution has
780 typically less predictive power in the extrapolated range. Including expert
781 estimates, weighted by their ability to estimate the 10-year discharges,
782 improved the precision in this range of extremes.

783 Several model choices were made to obtain these results. Their implications
784 warrant further discussion and substantiation. This section addresses the
785 choice for the elicited variables, the predictive power of 10-year discharge
786 estimates for 1000-year discharges, the overall credibility of the results,
787 and finally, some comments on model choices and uncertainty.

788 **5.1 Method and model choices**

789 We chose to elicit tributary discharges, rather than the downstream
790 discharges (our ultimate variable of interest) themselves. We believe that
791 experts' estimates for tributary discharges correspond better to catchment
792 hydrology (rainfall-runoff response). Additionally, this choice enables us to
793 validate the final result with the downstream discharges. With the chosen
794 set-up we thus test the experts' capabilities for estimating system discharge
795 extremes from tributary components, while still considering the catchment

796 hydrology, rather than just informing us with their estimates for the end
797 results. However, this does not guarantee that the downstream discharges
798 calculated from the experts' answers match the discharges they would have
799 given if elicited directly.

800 We fitted the GEV-distribution based on the elicited 10-year and 1000-year
801 discharges. In particular the GEV's uncertain tail shape parameter is
802 informed through this, as the location and scale parameter can be estimated
803 from data with relative certainty. Alternatively, we could have estimated
804 the tail shape parameter directly or estimated a related parameter such as
805 the ratio or difference between discharges. The latter was done by Renard,
806 Lang, and Bois (2006) who elicited the 10-year discharge and the
807 *differences* between the 10- and 100-year and 100- and 1,000-year
808 discharges. This approach reduces the dependence between expert
809 estimates for different quantiles, and therefore between the priors (when
810 more than one quantile is used) (Coles and Tawn 1996). Additionally, it
811 shifts the experts' focus to assessing how surprising or extreme rare events
812 can be. Because we were ultimately interested in the 1000-year discharges,
813 we chose eliciting this discharge directly. This will give a more accurate
814 representation of this specific value than composing it of two random
815 variables with a dependence that is unknown to us. We appreciate however
816 that if experts would have estimates ratios or differences, and been
817 evaluated by this, different weights would have resulted than the ones
818 presented in this research (refer to the markedly different ratios between
819 the 10-year and 1,000-year discharge for the two best experts D and E in
820 Fig. 5). A study focusing on how surprising large events can be, and whether
821 one method renders consistently larger estimates than the other, would
822 make an interesting comparison. Finally, we note that Renard, Lang, and
823 Bois (2006) combine different extreme value distributions with non-
824 stationary parameters in a single Bayesian analysis, which makes their
825 method a good example of incorporate climate change effects (often
826 considered a driver of for new extremes) in the method as well. This was
827 however out of the scope of our research, which shows that extreme
828 discharge statistics can be improved when combining them with structured
829 expert judgment procedures.

830 Regarding the goodness-of-fit of the chosen GEV distribution, we note that
831 some of the experts estimated 1,000-year discharges much higher of lower
832 than would be expected from observations. This might indicate that the
833 GEV-distribution is not the right model to observations and expert
834 estimates. However, a significantly lower estimate indicates that the
835 estimated discharge is wrong, as it is unlikely that the 1,000-year discharge
836 is lower than the highest on record. A significantly higher estimate, on the
837 other hand, might be valid, due to a belief in a change in catchment
838 response under extreme rainfall (e.g., due to a failing dam). This would
839 violate the GEV-distribution's 'identically distributed' assumption.

840 However, the GEV has sufficient shape flexibility to facilitate substantially
841 higher 1,000-year discharges, so we do not consider this a realistic
842 shortcoming. Accordingly, rather than viewing the GEV as a limiting factor
843 for fitting the data, we use it as a validation for the Classical Model scores,
844 as described in Sect. 5.2.

845 Finally, we note the model's omission of seasonality. The July 2021 event
846 was mainly extraordinary because of its magnitude *in combination with* the
847 fact that it happened during summer. Including seasonality would have
848 been a valuable addition to the model but it would also have (at least)
849 doubled the number of estimates provided by each expert, which was not
850 feasible for this study. The exclusion of seasonality from our research does
851 not alter our main conclusion, which is the possibility of enhancing
852 estimation of extreme discharges through structured expert judgments.

853 **5.2 Validity of the results**

854 The experts participating in this study were asked to estimate 10-year and
855 1000-year discharges. While both discharges are unknown to the expert,
856 the underlying processes leading to the different return period estimates
857 can be different. An implicit assumption is that the experts' ability to
858 estimate the seed variables (a 10-year discharge) reflects their ability to
859 estimate the target variables (a 1000-year discharge). This assumption is in
860 fact one of the most crucial assumptions in the Classical Model ~~and~~. [The](#)
861 [objective of this research is not to investigate this assumption. For an](#)
862 [example of a recent discussion on the effect of seed variables on the](#)
863 [performance of the Classical Model the reader is referred to \(Eggstaff,](#)
864 [Mazzuchi, and Sarkani 2014\). The representativeness of the seed variables](#)
865 [for calibration variables](#) has extensively been discussed in, for example,
866 (Roger M. Cooke 1991). Seed questions have to be as close as possible to the
867 variables of interest, and mostly concern similar questions from different
868 cases or studies. Precise 1000-year discharge estimates are however
869 unknown for any river system, making this option infeasible for this study.
870 In comparison, with a conventional model-based approach, the ability of a
871 model to predict extremes is also estimated from (and tailored to) the
872 ability to estimate historical observations (through calibration). Advantages
873 of relying in the extrapolation of a group of experts are that they can
874 explicitly consider uncertainty and are assessed on their ability to do so
875 through the Classical Model. In Sect. 5.1 we described how inconsistencies
876 between the observations and expert estimates can lead to a sub-optimal
877 GEV-fit. The fact that this is most prevalent in the low-scoring experts and
878 least for experts D and E supports the credibility of the results. Moreover,
879 this means that the 'bad' fits have little weight in the final global weight DM
880 results, and secondly that the GEV is considered a suitable statistical
881 distribution to fit observations and expert estimates.

882 The GRADE results from (Hegnauer and Van den Boogaard 2016) were
883 used to validate the 1,000-year downstream discharge results. These
884 GRADE-statistics at Borgharen (currently used for dike assessment) give a
885 lower and less uncertain range for the 1,000-year discharge than the
886 estimates obtained through our methodology. The estimates obtained in
887 this study present larger uncertainty bands and indicate higher extreme
888 discharges. This might be a consequence of the fact that we did not show
889 the measured tributary discharges to the experts, such that we could clearly
890 distinguish the effect of observations and ‘prior’ expert judgments.
891 Moreover, GRADE (at the time) did not include the July 2021 event. If the
892 GRADE statistics had been derived with the inclusion of the July 2021 event,
893 it would likely assign more probability to higher discharges. The
894 ~~experts~~experts’ estimates on the contrary were elicited after the July 2021
895 event which likely did affect their estimates. Therefore, the comparison
896 between GRADE and the expert estimates should not be used to assess
897 correctness, but as an indication of whether the results are in the right
898 range. Finally, note that the full GRADE-method is not published in a peer-
899 reviewed journal (the weather generator is, (Leander et al. 2005)).
900 However, because the results are widely used in the Dutch practice of flood
901 risk assessment (and known to the experts as well) we considered them the
902 best source for comparing the results in the present study.

903 To evaluate the value of the applied approach that uses data combined with
904 expert estimates, we compared the results that were fitted to only data or
905 only expert judgment to the results of the combination. For the last option
906 we used an equal weight decision maker, a conservative choice as the
907 experts’ statistical accuracy could potentially still be determined based on a
908 different river where data for seed questions are available. While the
909 marginal distributions of the EJ-only case present wide bandwidths (see
910 Fig. [fig:extreme_discharges_Borgharen] b and e), the final results for
911 Borgharen still gave a statistically accurate result but with a few caveats,
912 namely that the uncertainty is very large and that the 10-year and 1,000-
913 year estimates in itself are insufficient to inform the GEV without adding
914 prior information (otherwise we have 2 estimates for 3 parameters).
915 Consequently, when only using expert estimates, eliciting the random
916 variable (discharges) directly through a number of quantiles of interest,
917 might be a suitable alternative.

918 **5.3 Final remarks on model choices**

919 Finally, we note that using expert judgment to estimates discharges through
920 a model (like we did) still gives the analyst a large influence in the results.
921 We try to keep the model transparent and provide the experts with
922 unbiased information, but by defining the model on beforehand and
923 providing specific information we steer the participants towards a specific
924 way of reasoning. Every step in the method, such as the choice for a GEV-
925 distribution, the dependence model, or the choice for the Classical Model,

926 affects the end result. By presenting the method and providing background
927 information explicitly, we hope to have made this transparent and show the
928 usefulness of the method for similar applications.

929 **6 Conclusions**

930 This study sets out to establish a method for estimation of statistical
931 extremes through structured expert judgment and Bayesian inference, in a
932 case-study for extreme river discharges on the [Meuse](#) River-~~Meuse~~. Experts'
933 estimates of tributary discharges that are exceeded in a once per 10 year
934 and once per 1,000-year event are combined with high river discharges
935 measured over the past 30-70 years. We combine the discharges from
936 different tributaries with a multivariate correlation model describing their
937 dependence and compare the results for three approaches, a) data only, b)
938 expert judgment only, and c) the combination. The expert elicitation is
939 formalized with the Classical Model for structured expert judgment.

940 The results of applying our method show credible extreme river discharges
941 resulting from the combined expert-and-data approach. A comparison to
942 GRADE, the prevailing method for estimating discharge extremes on the
943 Meuse, gives similar ranges for the 10-, 100-, 1,000-year discharges as
944 GRADE. Moreover, the two experts with the highest scores from the
945 Classical Model had discharge estimates that correspond well with those
946 discharges that might be expected from the observations. This indicates
947 that using the Classical Model to assess expert performance is a suitable
948 way of using expert judgment to limit the uncertainty in the “out of sample”
949 range of extremes. The experts-only approach performs satisfactory as well,
950 albeit with a considerably larger uncertainty than the EJ-data option. The
951 method may also be applied to river systems where measurement data are
952 scarce or absent, but adding information on less extreme events is desirable
953 to increase the precision of the estimates.

954 On a broader level, this study has demonstrated the potential of combining
955 structured expert judgment and Bayesian analysis in informing priors and
956 reducing uncertainty in statistical models. When estimates on uncertain
957 extremes ~~is~~[are](#) needed, which cannot satisfactorily be derived (exclusively)
958 from a (limited) data-record, the presented approach provides a means [\(not](#)
959 [the only mean\)](#) of supplementing this information. Structured expert
960 judgment provides an approach of deriving defensible priors, while the
961 Bayesian framework offers flexibility for incorporating these into
962 probabilistic results by adjusting the likelihood of input or output
963 parameters. In our application to the Meuse River, we successfully elicited
964 credible extreme discharges. However, ~~a~~-case studies for different rivers
965 should verify these findings. [Our research does not discourages the use of](#)
966 [more traditional approaches such as rainfall-runoff or other hydrodynamic](#)
967 [or statistical models](#). Considering the credible results and the relatively

968 manageable effort required, the approach ~~presents~~(when well
969 ~~implemented) can present~~ an attractive alternative ~~for complex~~
970 ~~hydrological studies where the~~to models that approach uncertainty in
971 extremes ~~needs to be constrained~~in a less transparent way.

972 **Appendix A. Calculation of downstream discharges**

973 Section 3.4 explained the method applied and choices made for calculating
974 downstream discharges. This appendix explains this in more detail,
975 including the mathematical equations.

976 Three model components are elicited from the experts and data:

- 977 • Marginal tributary discharges, in the form of a MCMC GEV-
978 parameter trace. Each combination θ consists of a location (μ),
979 scale (σ), and tail-shape parameter (ξ).
- 980 • A ratio between the sum of upstream peak discharges and the
981 downstream peak discharge, represented by This is a single
982 probability distribution.
- 983 • The interdependence between tributary discharges, in the form of
984 a multivariate normal distribution.

985 The exceedance frequency curves for the downstream discharges are
986 calculated based on 9 tributaries (N_T), a trace of 10,000 MCMC parameter
987 combinations (N_M), and 10,000 discharge events (N_Q) per curve.

988 The N_M parameter combinations for each tributary are sorted based on the
989 (1,000-year) discharge with an exceedance probability of 0.001:
990 $F_{GEV}^{-1}(1 - 0.001|\theta)$, in which F_{GEV}^{-1} is the inverse cumulative density function,
991 or percentile point function, of the tributary GEV. Sorting the discharges
992 like this enables us to select parameter combinations that lead to low or
993 high discharges in multiple tributaries, and in this way express the
994 tributary correlations. The sorting order might be different for the 10-year
995 discharge than it is for the 1000-year discharge. The latter is however
996 chosen as it is most interesting for this study.

997 For calculating a single curve, N_T realizations are drawn from the
998 dependence model. These normally distributed realizations (\mathbf{x}) are
999 transformed to the $[1, N_M]$ interval, and are then used as index j to select a
1000 GEV-parameter combination for each of the N_T tributaries:

1001
$$j = \text{Round}(F_{norm}(\mathbf{x}) \cdot (N_M - 1) + 1).$$

1002 This is the first of two ways in which the interdependence between
1003 tributary discharges is expressed. The second is the next step, drawing a
1004 $(N_T \times N_Q)$ sample Y from the dependence model. These events (on a
1005 standard normal scale) are transformed to the discharge realizations Q for
1006 each ~~tributaries'~~ tributary's GEV parameter combination:

1007
$$Q = F_{GEV,j}^{-1}(F_{norm}(Y))$$

1008 An N_Q sized sample for the ratio between upstream sum and downstream
1009 discharges (f) is drawn as well. The ($N_T \times N_Q$) discharges Q are summed per
1010 event (for all tributaries), and multiplied with the factor f ,

$$1011 \quad q = f \cdot \sum(Q).$$

1012 Note that this notation corresponds to Eq. [\[eq:main_model\]](#). The N_Q
1013 discharges q are subsequently sorted and assigned a plot positions:

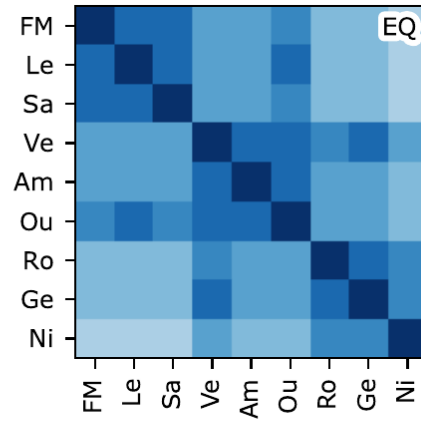
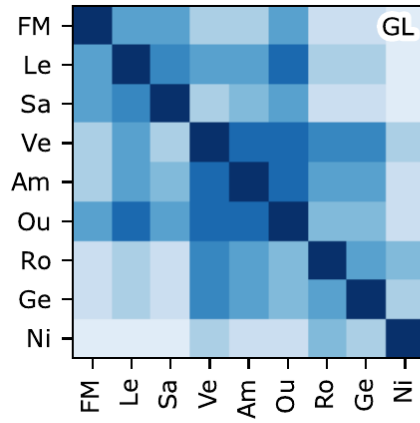
$$1014 \quad p = \frac{k - a}{N_Q + b},$$

1015 with a and b being the plot positions, 0.3 and 0.4, respectively (from
1016 Bernard and Bos-Levenbach 1955). k indicates the order of the events in
1017 the set (1 being the largest, N_Q the smallest), The plot positions (p) are the
1018 ‘empirical’ exceedance probabilities of the model. With 10,000 discharges
1019 and our exceedance probability of interest of 1/1,000, the results are
1020 insensitive to the choice of plot positions.

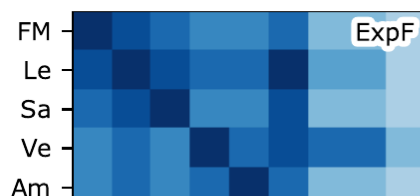
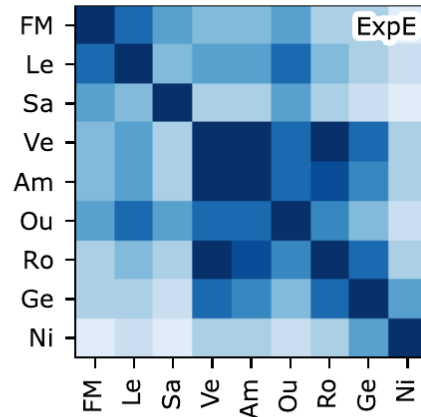
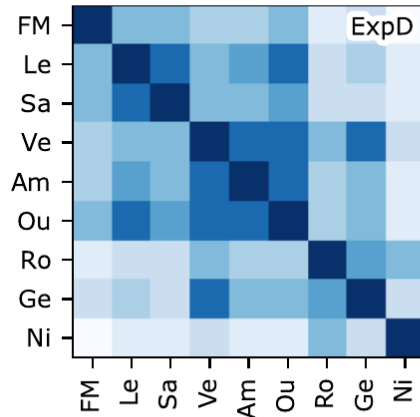
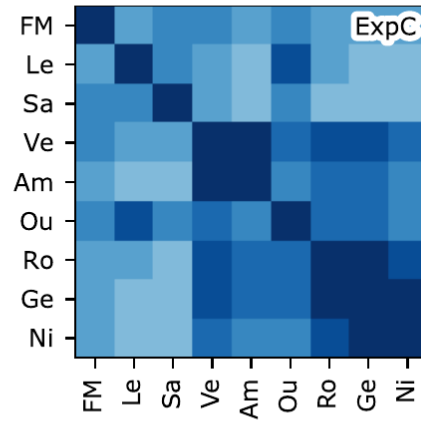
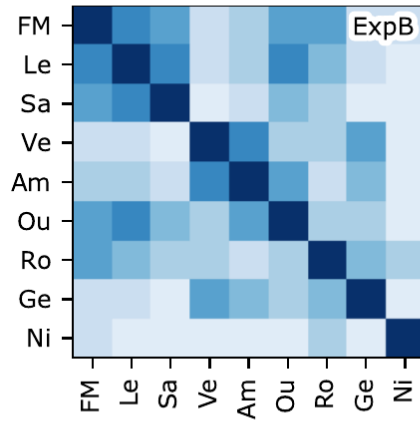
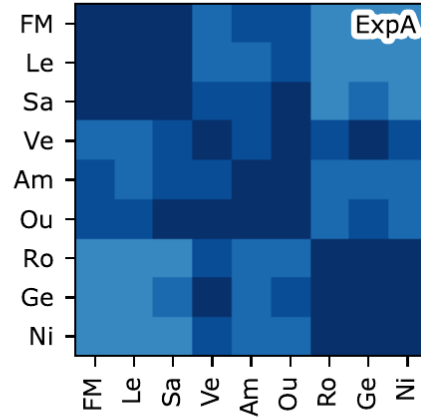
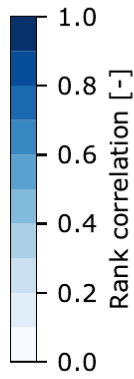
1021 This procedure results in one exceedance frequency curve for the
1022 downstream discharge. The procedure is repeated 10,000 times to generate
1023 [a an](#) uncertainty interval for the discharge estimate. Note that the full Monte
1024 Carlo simulation comprises $10,000 \times 10,000 = 100,000,000$ ‘events’ for the
1025 9 tributaries.

1026 **Appendix B. Expert and DM correlation matrices**

1027 Figure 7 shows the correlation matrices estimated by the experts. The DM
1028 correlation matrices are weighted combinations of the expert matrices,
1029 based on the weights from Table 1. See subsection 3.2 and equation
1030 [eq:DM].



FM: French Meuse
 Le: Lesse
 Sa: Sambre
 Ve: Vesdre
 Am: Ambleve
 Ou: Ourthe
 Ro: Roer
 Ge: Geul
 Ni: Niers



1032 *Figure 7: Correlation matrices estimated by the expert*

1033 We would like to thank all experts that participated in the study, Alexander,
1034 Eric, Ferdinand, Helena, Jerom, Nicole, and Siebolt, for their time and effort
1035 in making this research possible. Secondly, we thank Dorien Lugt en Ties
1036 van der Heijden, who's hydrological and statistical expertise greatly helped
1037 in preparing the study through test rounds.

1038 This research was funded by the TKI project EMU-FD. This research project
1039 is funded by Rijkswaterstaat, Deltares and HKV consultants.

1040 **7 References**

1041 Al-Awadhi, Shafeeqah A, and Paul H Garthwaite. 1998. "An Elicitation
1042 Method for Multivariate Normal Distributions." *Communications in*
1043 *Statistics-Theory and Methods* 27 (5): 1123–42.

1044 Bamber, Jonathan L, Michael Oppenheimer, Robert E Kopp, Willy P Aspinall,
1045 and Roger M Cooke. 2019. "Ice Sheet Contributions to Future Sea-Level Rise
1046 from Structured Expert Judgment." *Proceedings of the National Academy of*
1047 *Sciences* 116 (23): 11195–200.

1048 Benito, Gerardo, and VR Thorndycraft. 2005. "Palaeoflood Hydrology and
1049 Its Role in Applied Hydrological Sciences." *Journal of Hydrology* 313 (1-2):
1050 3–15.

1051 Bernard, A, and EJ Bos-Levenbach. 1955. "The Plotting of Observations on
1052 Probability-Paper." *Stichting Mathematisch Centrum. Statistische Afdeling*,
1053 no. SP 30a/55.

1054 Boer-Euser, Tanja de, Laurène Bouaziz, Jan De Niel, Claudia Brauer,
1055 Benjamin Dewals, Gilles Drogue, Fabrizio Fenicia, et al. 2017. "Looking
1056 Beyond General Metrics for Model Comparison—Lessons from an
1057 International Model Intercomparison Study." *Hydrology and Earth System*
1058 *Sciences* 21 (1): 423–40.

1059 Bouaziz, Laurène JE, Guillaume Thirel, Tanja de Boer-Euser, Lieke A Melsen,
1060 Joost Buitink, Claudia C Brauer, Jan De Niel, et al. 2020. "Behind the Scenes
1061 of Streamflow Model Performance." *Hydrology and Earth System Sciences*
1062 *Discussions* 2020: 1–38.

1063 Brázdil, Rudolf, Zbigniew W Kundzewicz, Gerardo Benito, Gaston Demarée,
1064 Neil Macdonald, Lars A Roald, et al. 2012. "Historical Floods in Europe in
1065 the Past Millennium." *Changes in Flood Risk in Europe, Edited by:*
1066 *Kundzewicz, ZW, IAHS Press, Wallingford, 121–66.*

- 1067 Coles, Stuart G, and Jonathan A Tawn. 1996. "A Bayesian Analysis of
1068 Extreme Rainfall Data." *Journal of the Royal Statistical Society: Series C*
1069 *(Applied Statistics)* 45 (4): 463–78.
- 1070 Colson, Abigail R, and Roger M Cooke. 2017. "Cross Validation for the
1071 Classical Model of Structured Expert Judgment." *Reliability Engineering &*
1072 *System Safety* 163: 109–20.
- 1073 Cooke, Roger M. 1991. *Experts in Uncertainty: Opinion and Subjective*
1074 *Probability in Science*. Oxford University Press, USA.
- 1075 Cooke, Roger M., and Louis L. H. J. Goossens. 2008. "TU Delft expert
1076 judgment data base." *Reliability Engineering and System Safety* 93 (5): 657–
1077 74. <https://doi.org/10.1016/j.ress.2007.03.005>.
- 1078 [Cooke, Roger M, Deniz Marti, and Thomas Mazzuchi. 2021. "Expert](#)
1079 [Forecasting with and Without Uncertainty Quantification and Weighting:](#)
1080 [What Do the Data Say?" *International Journal of Forecasting* 37 \(1\): 378–87.](#)
- 1081 Copernicus Land Monitoring Service. 2017. "EU-DEM."
1082 <https://land.copernicus.eu/imagery-in-situ/eu-dem/eu-dem-v1.1/view>.
- 1083 ———. 2018. "CORINE Land Cover." [https://land.copernicus.eu/pan-](https://land.copernicus.eu/pan-european/corine-land-cover/clc2018?tab=download)
1084 [european/corine-land-cover/clc2018?tab=download](https://land.copernicus.eu/pan-european/corine-land-cover/clc2018?tab=download).
- 1085 ———. 2020. "E-OBS."
1086 [https://cds.climate.copernicus.eu/cdsapp#!/dataset/insitu-gridded-](https://cds.climate.copernicus.eu/cdsapp#!/dataset/insitu-gridded-observations-europe?tab=overview)
1087 [observations-europe?tab=overview](https://cds.climate.copernicus.eu/cdsapp#!/dataset/insitu-gridded-observations-europe?tab=overview).
- 1088 De Niel, J, G. Demarée, and P. Willems. 2017. "Weather Typing-Based Flood
1089 Frequency Analysis Verified for Exceptional Historical Events of Past 500
1090 Years Along the Meuse River." *Water Resources Research* 53 (10): 8459–74.
1091 <https://doi.org/https://doi.org/10.1002/2017WR020803>.
- 1092 Dewals, Benjamin, Sébastien Erpicum, Michel Piroton, and Pierre
1093 Archambeau. 2021. "Extreme floods in Belgium. The July 2021 extreme
1094 floods in the Belgian part of the Meuse basin."
- 1095 [Dimitriadis, Panayiotis, Demetris Koutsoyiannis, Theano Iliopoulou, and](#)
1096 [Panos Papanicolaou. 2021. "A Global-Scale Investigation of Stochastic](#)
1097 [Similarities in Marginal Distribution and Dependence Structure of Key](#)
1098 [Hydrological-Cycle Processes." *Hydrology* 8 \(2\).](#)
1099 <https://doi.org/10.3390/hydrology8020059>.
- 1100 Dion, Patrice, Nora Galbraith, and Elham Sirag. 2020. "Using Expert
1101 Elicitation to Build Long-Term Projection Assumptions." In *Developments in*
1102 *Demographic Forecasting*, 43–62. Springer, Cham.

- 1103 [Eggstaff, Justin W., Thomas A. Mazzuchi, and Shahram Sarkani. 2014. "The](#)
1104 [Effect of the Number of Seed Variables on the Performance of Cooke's](#)
1105 [Classical Model." *Reliability Engineering & System Safety* 121: 72–82.](#)
1106 <https://doi.org/https://doi.org/10.1016/j.ress.2013.07.015>.
- 1107 Food and Agriculture Organization of the United Nations. 2003. "Digital Soil
1108 Map of the World."
1109 [https://data.apps.fao.org/map/catalog/srv/eng/catalog.search?id=14116#](https://data.apps.fao.org/map/catalog/srv/eng/catalog.search?id=14116#/metadata/446ed430-8383-11db-b9b2-000d939bc5d8)
1110 [/metadata/446ed430-8383-11db-b9b2-000d939bc5d8](https://data.apps.fao.org/map/catalog/srv/eng/catalog.search?id=14116#/metadata/446ed430-8383-11db-b9b2-000d939bc5d8).
- 1111 Foreman-Mackey, Daniel, David W. Hogg, Dustin Lang, and Jonathan
1112 Goodman. 2013. "emcee: The MCMC Hammer." *Publications of the*
1113 *Astronomical Society of the Pacific* 125 (925): 306.
1114 <https://doi.org/10.1086/670067>.
- 1115 Goodman, Jonathan, and Jonathan Weare. 2010. "Ensemble Samplers with
1116 Affine Invariance." *Communications in Applied Mathematics and*
1117 *Computational Science* 5 (1): 65–80.
- 1118 Hanea, Anca, Oswaldo Morales Napoles, and Dan Ababei. 2015. "Non-
1119 Parametric Bayesian Networks: Improving Theory and Reviewing
1120 Applications." *Reliability Engineering & System Safety* 144: 265–84.
1121 <https://doi.org/https://doi.org/10.1016/j.ress.2015.07.027>.
- 1122 Hart, Cornelis Marcel Pieter 't, Georgios Leontaris, and Oswaldo Morales-
1123 Nápoles. 2019. "Update (1.1) to ANDURIL — a MATLAB Toolbox for
1124 ANalysis and Decisions with Uncertainty: Learning from Expert Judgments:
1125 ANDURYL." *SoftwareX* 10: 100295.
1126 <https://doi.org/https://doi.org/10.1016/j.softx.2019.100295>.
- 1127 Hegnauer, M, JJ Beersma, HFP Van den Boogaard, TA Buishand, and RH
1128 Passchier. 2014. "Generator of Rainfall and Discharge Extremes (GRADE)
1129 for the Rhine and Meuse basins. Final report of GRADE 2.0." Delft: Deltares.
- 1130 Hegnauer, M, and HFP Van den Boogaard. 2016. "GPD verdeling in de
1131 GRADE onzekerheidsanalyse voor de Maas." Delft: Deltares.
- 1132 Jenkinson, A. F. 1955. "The Frequency Distribution of the Annual Maximum
1133 (or Minimum) Values of Meteorological Elements." *Quarterly Journal of the*
1134 *Royal Meteorological Society* 81 (348): 158–71.
1135 <https://doi.org/https://doi.org/10.1002/qj.49708134804>.
- 1136 Keelin, Thomas W. 2016. "The Metalog Distributions." *Decision Analysis* 13
1137 (4): 243–77.
- 1138 Kindermann, Paulina E, Wietske S Brouwer, Amber van Hamel, Mick van
1139 Haren, Rik P Verboeket, Gabriela F Nane, Hanik Lakhe, Rajaram Prajapati,
1140 and Jeffrey C Davids. 2020. "Return Level Analysis of the Hanumante River

- 1141 Using Structured Expert Judgment: A Reconstruction of Historical Water
1142 Levels." *Water* 12 (11): 3229.
- 1143 [Koutsoyiannis, Demetris. 2004a. "Statistics of Extremes and Estimation of](#)
1144 [Extreme Rainfall: I. Theoretical Investigation / Statistiques de Valeurs](#)
1145 [Extrêmes Et Estimation de Précipitations Extrêmes: I. Recherche](#)
1146 [Théorique." *Hydrological Sciences Journal* 49 \(4\): -590.](#)
1147 <https://doi.org/10.1623/hysj.49.4.575.54430>.
- 1148 [———. 2004b. "Statistics of Extremes and Estimation of Extreme Rainfall:](#)
1149 [II. Empirical Investigation of Long Rainfall Records / Statistiques de Valeurs](#)
1150 [Extrêmes Et Estimation de Précipitations Extrêmes: II. Recherche](#)
1151 [Empirique Sur de Longues Séries de Précipitations." *Hydrological Sciences*](#)
1152 [Journal](#) 49 (4): -610. <https://doi.org/10.1623/hysj.49.4.591.54424>.
- 1153 Land NRW. 2022. "ELWAS-WEB." <https://www.elwasweb.nrw.de/elwas->
1154 [web/index.xhtml#](https://www.elwasweb.nrw.de/elwas-web/index.xhtml#).
- 1155 Langemheen, W. van de, and H. E. J. Berger. 2001. "Hydraulische
1156 Randvoorwaarden 2001: Maatgevende Afvoeren Rijn En Maas." RIZA;
1157 Ministerie van Verkeer en Waterstaat.
- 1158 Leander, Robert, Adri Buishand, Paul Aalders, and Marcel De Wit. 2005.
1159 "Estimation of extreme floods of the River Meuse using a stochastic weather
1160 generator and a rainfall." *Hydrological Sciences Journal* 50 (6).
- 1161 Leontaris, Georgios, and Oswaldo Morales-Nápoles. 2018. "ANDURIL — a
1162 MATLAB Toolbox for ANalysis and Decisions with UnceRtaInty: Learning
1163 from Expert Judgments." *SoftwareX* 7: 313–17.
1164 <https://doi.org/https://doi.org/10.1016/j.softx.2018.07.001>.
- 1165 Marti, Deniz, Thomas A. Mazzuchi, and Roger M. Cooke. 2021. "Are
1166 Performance Weights Beneficial? Investigating the Random Expert
1167 Hypothesis." *Expert Judgement in Risk and Decision Analysis* 293: 53–82.
1168 https://doi.org/10.1007/978-3-030-46474-5_3.
- 1169 Martins, Eduardo S, and Jery R Stedinger. 2000. "Generalized Maximum-
1170 Likelihood Generalized Extreme-Value Quantile Estimators for Hydrologic
1171 Data." *Water Resources Research* 36 (3): 737–44.
- 1172 Ministry of Infrastructure and Environment. 2016. "Regeling Veiligheid
1173 Primaire Waterkeringen 2017 No IENM/BSK-2016/283517."
- 1174 Mohr, Susanna, Uwe Ehret, Michael Kunz, Patrick Ludwig, Alberto Caldas-
1175 Alvarez, James E Daniell, Florian Ehmele, et al. 2022. "A Multi-Disciplinary
1176 Analysis of the Exceptional Flood Event of July 2021 in Central Europe. Part
1177 1: Event Description and Analysis." *Natural Hazards and Earth System*
1178 *Sciences Discussions*, 1–44.

- 1179 Oppenheimer, Michael, Christopher M Little, and Roger M Cooke. 2016.
1180 “Expert Judgement and Uncertainty Quantification for Climate Change.”
1181 *Nature Climate Change* 6 (5): 445–51.
- 1182 Papalexiou, Simon Michael, and Demetris Koutsoyiannis. 2013. “Battle of
1183 Extreme Value Distributions: A Global Survey on Extreme Daily Rainfall.”
1184 *Water Resources Research* 49 (1): 187–201.
- 1185 Parent, Eric, and Jacques Bernier. 2003. “Encoding Prior Experts Judgments
1186 to Improve Risk Analysis of Extreme Hydrological Events via POT
1187 Modeling.” *Journal of Hydrology* 283 (1-4): 1–18.
- 1188 Renard, Benjamin, Michel Lang, and Philippe Bois. 2006. “Statistical
1189 Analysis of Extreme Events in a Non-Stationary Context via a Bayesian
1190 Framework: Case Study with Peak-over-Threshold Data.” *Stochastic
1191 Environmental Research and Risk Assessment* 21 (2): 97–112.
- 1192 Rijkswaterstaat. 2022. “Waterinfo.”
1193 [https://waterinfo.rws.nl/#!/kaart/Afvoer/Debiet__20Oppervlaktewater__](https://waterinfo.rws.nl/#!/kaart/Afvoer/Debiet__20Oppervlaktewater__20m3__2Fs/)
1194 [20m3__2Fs/](https://waterinfo.rws.nl/#!/kaart/Afvoer/Debiet__20Oppervlaktewater__20m3__2Fs/).
- 1195 Rongen, G, O Morales-Nápoles, and M Kok. 2022a. “Expert Judgment-Based
1196 Reliability Analysis of the Dutch Flood Defense System.” *Reliability
1197 Engineering & System Safety* 224: 108535.
- 1198 ———. 2022b. “Extreme Discharge Uncertainty Estimates for the River
1199 Meuse Using a Hierarchical Non-Parametric Bayesian Network.” In
1200 *Proceedings of the 32th European Safety and Reliability Conference (ESREL
1201 2022)*, edited by Maria Chiara Leva, Edoardo Patelli, Luca Podofillini, and
1202 Simon Wilson, 2670–77. Research Publishing.
1203 https://doi.org/10.3850/978-981-18-5183-4_S17-04-622-cd.
- 1204 Rongen, Guus, Cornelis Marcel Pieter ’t Hart, Georgios Leontaris, and
1205 Oswaldo Morales-Nápoles. 2020. “Update (1.2) to ANDURIL and ANDURL:
1206 Performance Improvements and a Graphical User Interface.” *SoftwareX* 12:
1207 100497. <https://doi.org/https://doi.org/10.1016/j.softx.2020.100497>.
- 1208 Rongen, GWF. 2016. “The effect of flooding along the Belgian Meuse on the
1209 discharge and hydrograph shape at Eijsden.” Master’s thesis, Delft
1210 University of Technology; Delft University of Technology.
- 1211 Sebok, Eva, Hans Jørgen Henriksen, Ernesto Pastén-Zapata, Peter Berg,
1212 Guillume Thirel, Anthony Lemoine, Andrea Lira-Loarca, et al. 2021. “Use of
1213 Expert Elicitation to Assign Weights to Climate and Hydrological Models in
1214 Climate Impact Studies.” *Hydrology and Earth System Sciences Discussions*,
1215 1–35.

- 1216 Service public de Wallonie. 2022. "Annaires Et Statistiques." [http://voies-](http://voies-hydrauliques.wallonie.be/opencms/opencms/fr/hydro/Archive/annuaires/index.html)
1217 [hydrauliques.wallonie.be/opencms/opencms/fr/hydro/Archive/annuaires](http://voies-hydrauliques.wallonie.be/opencms/opencms/fr/hydro/Archive/annuaires/index.html)
1218 [/index.html](http://voies-hydrauliques.wallonie.be/opencms/opencms/fr/hydro/Archive/annuaires/index.html).
- 1219 TFFF. 2021. "Hoogwater 2021 - Feiten en duiding." Delft: Task Force Fact-
1220 finding hoogwater 2021; Expertisenetwerk Waterveiligheid (ENW).
- 1221 Viglione, Alberto, Ralf Merz, José Luis Salinas, and Günter Blöschl. 2013.
1222 "Flood Frequency Hydrology: 3. A Bayesian Analysis." *Water Resources*
1223 *Research* 49 (2): 675–92.
- 1224 Waterschap Limburg. 2021. "Discharge Measurements."